Using repeat electrical resistivity surveys to assess heterogeneity in soil moisture dynamics under contrasting vegetation types

Jonathan Dick[1, 5], Doerthe Tetzlaff[1,2,3], John Bradford[4], Chris Soulsby[1]

[1]Northern Rivers Institute, University of Aberdeen, Aberdeen, UK (j.j.dick@ljmu.ac.uk)

[2] IGB Leibniz Institute of Freshwater Ecology and Inland Fisheries
[3] Humboldt University Berlin
[4]Colarado School of Mines
[5]Liverpool John Moores University

Abstract

As the relationship between vegetation and soil moisture is complex and reciprocal, there is a need to understand how spatial patterns in soil moisture influence the distribution of vegetation, and how the structure of vegetation canopies and root networks regulates the partitioning of precipitation. Spatial patterns of soil moisture are often difficult to visualise as usually, soil moisture is measured at point scales, and often difficult to extrapolate. Here, we address the difficulties in collecting large amounts of spatial soil moisture data through a study combining plot- and transect-scale electrical resistivity tomography (ERT) surveys to estimate soil moisture in a 3.2 km^2 upland catchment in the Scottish Highlands. The aim was to assess the spatio-temporal variability in soil moisture under Scots pine forest (*Pinus sylvestris*) and heather moorland shrubs (*Calluna* vulgaris); the two dominant vegetation types in the Scottish Highlands. The study focussed on one year of fortnightly ERT surveys. The surveyed resistivity data was inverted and Archie's law was used to calculate volumetric soil moisture by estimating parameters and comparing against field measured data. Results showed that spatial soil moisture patterns were more heterogeneous in the forest site, as were patterns of wetting and drying, which can be linked to vegetation distribution and canopy structure. The heather site showed a less heterogeneous response to wetting and drying, reflecting the more uniform vegetation cover of the shrubs. Comparing soil moisture temporal variability during growing and non-growing seasons revealed further contrasts: under the heather there was little change in soil moisture during the

28 growing season. Greatest changes in the forest were in areas where the trees were concentrated
29 reflecting water uptake and canopy partitioning. Such differences have implications for climate and
30 land use changes; increased forest cover can lead to greater spatial variability, greater growing season
31 temporal variability, and reduced levels of soil moisture, whilst projected decreasing summer
32 precipitation may alter the feedbacks between soil moisture and vegetation water use and increase
33 growing season soil moisture deficits.

34

35 **Keywords:** Electrical resistivity tomography; soil moisture; forest; moorland

36

37 **1. Introduction**

38 Soil moisture is a fundamental, highly dynamic, characteristic of terrestrial ecosystems, which
39 regulates vegetation productivity (Rodríguez-Iturbe and Porporato, 2007) and strongly influences
40 biogeochemical processes (Robinson et al., 2008). The relationship between vegetation cover and soil
41 moisture is complex (Entekhabi et al., 1996; Zribi et al., 2010). Soil moisture as the primary source of
42 water to plants commonly affects vegetation distribution (Stephenson 1990; Rodriguez-Iturbe et al.,
43 1999). In turn, the structure of vegetation canopies regulates water partitioning into interception
44 losses, and net precipitation as through-fall and stem flow (Helvey and Patric, 1965; Ford and Deans,
45 1978; Pypker et al., 2005). Spatial differences in inputs, together with complex patterns of water
46 uptake from highly distributed root networks, often create marked heterogeneity in soil moisture
47 distribution and associated dynamics (Liang et al., 2011; Coenders-Gerrits et al., 2013).

48 A changing climate is likely to alter the spatial and temporal dynamics of soil moisture in many areas
49 and this may, in turn, affect plant distribution and growth (Rodriguez-Iturbe et al., 1999; Seneviratne
50 et al., 2010). Climate change projections in many northern maritime regions infer a shift in

precipitation distributions towards increased winter inputs but reduced growing season rainfall (Murphy et al., 2009). With projected increased temperatures, this could result in potential water stresses during growing seasons in many regions (Reyer et al., 2013), which may lead to shifting vegetation patterns (Porporato et al., 2004; Rigling et al., 2013). With differences in water partitioning between vegetation types, it is important to understand how potential climatic and vegetation changes will affect the soil moisture in the landscape.

Measuring soil moisture at the point scale is relatively easy, however, marked heterogeneity in the subsurface (Cosh et al., 2004) dictates that it is difficult to upscale to landscape-scale processes (i.e. point to plot or hillslope or catchment scale) (Vereecken et al., 2008; Brocca et al., 2012; Tetzlaff et al., 2014). Heterogeneity in the subsurface also leads to spatial differences in soil moisture, something which may not be easily visualised using point measurements. Whilst there has been some success in using multiple point measurements to study the effects of vegetation on soil moisture (e.g. Teuling et al., 2006) there remains a need to assess processes occurring at larger scales and link these to vegetation-water interactions more clearly. New technologies such as cosmic ray sensors have potential in working passively over large areas to collect real-time data (Zreda et al., 2008), and have been successfully used to image field scale root zone soil moisture (Peterson et al., 2016). Unfortunately, their use is limited when considering small scale soil moisture patterns, as their spatial resolution is low (Zreda et al., 2008) Over the past few decades, geophysical techniques such as electrical resistivity tomography (ERT) have proven to be useful in estimating the soil moisture content of the vadose zone. Successful studies have used 2D transects (e.g. Schwartz et al., 2008; Brunet et al., 2010; Ain-Lhout et al., 2016) and 3D plots (e.g. al Hagrey, 2007; Srayeddin et al., 2009; Garré et al., 2011; Beff et al., 2013; Boaga et al., 2013; Chambers et al., 2014) to gain insight into soil moisture distributions.

ERT has great potential for understanding soil moisture variations at the plot and hillslope scale, and the way in which this variability is affected by vegetation (Zhou et al., 2001). Archie's law (Archie 1942) is commonly used to estimate soil moisture from electrical resistivity measurements (e.g. Zhou et al, 2001; Brunet et al, 2010; Schwartz et al, 2008). Specifically, Archie's law relates the electrical conductivity of a granular rock to its porosity, saturation and fluid conductivity. Difficulties in the use of Archie's law arise from the requirement to measure and estimate these variables and parameters, something essential when using ERT to estimate soil moisture. These parameters can be obtained from measurements conducted in the field (Zhou et al., 2001), lab (Brunet et al., 2010), or both (Schwartz et al. 2008).

Here, we use ERT to estimate soil moisture dynamics in a catchment in the Scottish Highlands, which is broadly representative of northern, formerly glaciated landscapes (Soulsby et al., 2015). Two soil-vegetation units dominate the catchment, namely shrub and forest vegetation on freely draining podzolic soils. Previous empirical and modelling studies have used hydrometric and tracer data to infer significant groundwater stores in drift aquifers (e.g. Soulsby et al., 2007; Birkel et al., 2010; Tetzlaff et al., 2014). Soulsby et al. (2016) previously used spatially distributed ERT surveys to characterise the distribution, thickness and properties (including water content) of extended glacial drifts in the study catchment. Here, we build on this work and seek to test the hypothesis that the influence of vegetation on spatial volumetric soil moisture patterns and dynamics will be different under heather and forest vegetation types due to the canopy structure and distribution of vegetation.

Our specific objectives were to:

(a) Estimate plot scale soil moisture from repeat plot- and transect-scale ERT measurements using the generalised Archie's law and time-domain reflectometry (TDR) soil moisture measurements

(b) Assess the spatial and temporal soil moisture heterogeneity within the rooting zone of the forest and heather sites to investigate the differences between vegetation types.

2. Study site

The study catchment, the Bruntland Burn (3.2 km^2) in NE Scotland, is described elsewhere in detail (Tetzlaff et al., 2014; Dick et al., 2014). Elevations range from 248 to 539 m.a.s.l, with mean slopes of 13°. The bedrock geology is predominantly granitic, bordered by schist and other metamorphic rocks in the south/southeast. The area was glaciated during the last glacial maximum, and as a result has a subdued topography with a wide flat valley bottom. The landscape is drift-draped, with shallow drift on the upper hillslopes grading to deeper glacial fills in the valley bottom (up to 40 m deep - Soulsby et al, 2016). The soils in the catchment are typical of these environments, with freely draining rankers and podzolic soils on the hillslopes, and more hydrologically responsive gleys (on the lower hillslopes) and deep peats (Histosols), up to 4 m deep, in the flat valley bottoms.

The vegetation is representative of many UK upland catchments. It is heavily influenced by historic land management practices with a long history of forest clearance, overgrazing by deer (*Cervus elaphus*) and sheep (*Ovis aries*), and moorland burning for grouse (*Lagopus lagopus*). As such, vegetation is dominated by heather shrubs (e.g. *Calluna vulgaris, Erica tetralix*) and grass (*Molinia caerulea*) moorland vegetation on the freely draining podzolic hillslopes and rankers. Due to the aforementioned land management practices, forest coverage is typically low, with mainly Scots Pine (*Pinus sylvestris*) on freely draining podzolic soils (Fig 1). Forests are focussed on areas where deer are excluded.

Two experimental locations were chosen in characteristic areas and both are representative of the dominant soil-vegetation units in the catchment (Fig 1). Both locations were in close proximity to long-term soil moisture measurement sites. One site was chosen under forest vegetation and one in the

heather moorland, both on podzolic soils. The heather site was located on the southwest side near the catchment outlet, and was situated on a topographically flat location (with some small micro-topography at the cm scale). The heather is around 0.2-0.3 m tall with 95% of roots in the upper 0.2 m of the soil profile (Sprenger et al.,, 2017), with a fairly dense and low canopy. In the heather, 21% of the precipitation is lost to interception. Transpiration in the heather site is estimated as 97 mm during the growing season (Wang et al., 2017). At the forest site, 95% of Scots Pine roots are contained within the upper 0.48 m of the soil profile (Haria and Price, 2000), and average canopy cover is 68%, varying between 20% and 90%, (Soulsby et al., 2017) (Fig 2). Around 45% of the gross precipitation is lost to interception (Wang et al., 2017). Transpiration estimates suggest 111 mm of transpired water during the growing season (derived from sap flow measurements between mid-April-early September; Wang et al., 2017).

3. Data and Methods

3.1 Hydrometric data

Meteorological data is required for temperature correction of electrical resistivity to a standard temperature, for which data primarily came from two sources, with hourly soil and air temperature data (to temperature-correct the resistivity data) from the MetOffice Aboyne No.2 station 20km away, through the British Atmospheric Data Centre (BADC). Soil temperature was averaged over the first 0.5 m of the soil profile. This data was supplemented with air temperature data from an automatic weather station situated in the Bruntland Burn, where precipitation and net radiation were measured every 15 minutes. The data from the AWS was then used to calculate PET using the method of Dunn and Mackay (1995).

Each of the study locations was instrumented for VSM measurements consisting of one soil moisture station per location. Each station was equipped for measuring VSM at 15 minutes intervals using

Campbell Scientific CS616 probes (c.f. Mittelbach et al., 2012) connected to a CR800X data logger. The same installation setup was used at each location and was described in detail by Geris et al. (2015). Probes were installed horizontally at 3 depths (0.15, 0.2 and 0.5 m) corresponding to the O, E, and B soil horizons, with two probes at each depth, with the VSM from both averaged. This was carried out to provide a replicate and account for subsurface heterogeneity, something which can lead to variable TDR VSM measurements. While CS616 probes are useful in collecting high temporal resolution datasets, there are potential problems associated with installation in stone rich soils, with measurements rods needing to remain the same distance apart and in contact with the surrounding soil. This can lead to problems when attempting to install spatially dense arrays for soil moisture measurement.

3.2 Electrical resistivity tomography

We collected ERT data using an IRIS instruments SysCal Pro 72 electrode system. An electrical current was injected through two of the electrodes (the source), and the potential difference was then measured between two other electrodes (Zonge et al., 2005; Binley et al., 2015). This was then repeated automatically, with different separations between the electrodes, depending on array and measurement length. We considered that when the electrodes are further apart, a greater proportion of the current flows deeper into the earth and, consequently, is influenced by deeper structures in the subsurface, and not just the surface.

At the forest site, one 7 by 8 m plot, and one 8.75 m transect were installed. At the heather site, one 3.5 by 4 m plot and one 8.75 m transect was installed. The forest plot was situated north of the catchment outlet, and was the topographically more variable site (surface elevation range: 0.9 m) (Fig 1). For all surveys, a dipole-dipole array was used, as this is more sensitive to lateral changes (Zonge et al., 2005), which is of interest when investigating spatial changes in soil moisture. While the better

signal to noise ratio of Wenner and Wenner-Schlumberger arrays would have been desirable, the inability to run these over multiple channels, and increased survey time made it impractical.

For the plot surveys, we placed 72 electrodes in a 8x9 node rectangular grid to visualise plot scale spatial VSM down to 0.5 m depths. A 3D orthogonal array was used, and was created using the Electre Pro software from Iris Instruments. All plot surveys used 6 stacks and 800 maximum voltage and a transmit time of 1000 ms. A 1 m grid spacing was used in the forest location, and a 0.5 m grid spacing in the heather location, giving mesh sizes of 0.5 m and 0.25 m respectively. The different spacing between the two plots was used to increase the resolution in the heather site because of the smaller size of the vegetation and the shallower root zone at that site. It must be noted that the difference in electrode spacing between surveys changes the resolution of the survey, as the resolution of an array is closely linked to the distance between the receiving and transmitting electrodes, with smaller distances increasing the resolution. This was deemed to be a reasonable trade-off as it increased the useful information gained with the higher resolution. The electrodes were 0.05 m x 0.05 m rectangular stainless-steel mesh (Tomaškovičová et al., 2016), and placed permanently by burying 0.05 m below the surface (Fig 1). These electrodes were chosen as the rocky subsurface made achieving a good contact difficult when using standard metal pegs. All plot data were collected for 6 depth levels corresponding to theoretical investigation depths of 0.7 m and 1.4 m in the heather and forest respectively, with an orthogonal survey pattern (Chambers et al., 2002). They were measured roughly fortnightly from October 2015 to September 2016 making a total of 21 surveys.

Alongside the plot ERT surveys, 9 transect surveys were also conducted at each site during the growing season (Mid-April to end of September). The ERT measurements were carried out at each of the sites with 36 electrodes and an electrode spacing of 0.25 m and 5 depth levels corresponding to an investigation depth of 1.85 m. Electrodes were 0.22 m long, ow which 0.1m penetrated the ground. As with the plots, surveys used 6 stacks and 800 maximum voltage and a transmit time of 1000 ms. The inversion mesh size was equal to the spacing. The transects were surveyed to provide higher

resolution insights of the VSM in the rooting zones of both the heather and forest because the existing resolution of the plot measurements was too coarse to adequately image the root zone anomaly, something which we wished to further investigate. This setup was chosen to focus on individual trees in the forest site, and for it to be logistically possible to do all four surveys on the same day.

Additionally, a larger transect was surveyed across the forest site to investigate the deeper subsurface under trees and to add context to the plot and smaller transect measurements. This transect was 72 m long, with a 1 m electrode spacing, and was surveyed at 9 depths with a theoretical investigation depth of 14 m. As with the smaller transects described above, the electrodes used were 0.22 m steel pegs.

After the surveys were completed, all data were pre-processed to remove erroneous measurements with anomalously high apparent resistivity values (>4000 Ωm) and high deviations of apparent resistivity (>0.5 Ωm) based on the quality index of the Syscal instrument. The filtered data were then corrected to 25 ^{o}C using the power function correction model of Besson et al. (2008)(Ma et al., 2011). Topography was incorporated during the pre-processing (from a survey of the sites using a total station when the arrays were installed). The measured resistivity data were then inverted using the standard least-squares constraint method in Geotomo Software's Res2dinv and Res3dinv.

3.3 Volumetric soil moisture estimation and analysis

Archie's law (Archie 1942) is commonly used to estimate soil moisture from electrical resistivity measurements (e.g. Zhou et al, 2001; Brunet et al, 2010; Schwartz et al, 2008). Specifically, Archie's law relates the electrical conductivity of a granular rock to its porosity, saturation and fluid conductivity.

There are several challenges in using ERT to estimate soil moisture, which still persist, even when partially mitigated using the generalised formula of Archie's law (Shah and Singh, 2005; Glover, 2010). In the use of this, there is still the requirement to estimate the m exponent parameter (which links

the pore network of the material to the resistivity) and include the pore water resistivity. These parameters and variables can be obtained from field measurements (Zhou et al., 2001), lab measurements (Brunet et al., 2010), or both (Schwartz et al., 2008). Still, even with field estimation of the parameters and variables, their estimation brings uncertainty, which can be controlled through the verification of estimated soil moisture against field measured soil moisture (e.g. Brillante et al., 2015). This approach has led to it being successfully employed in visualising vegetation-water interactions in agricultural (e.g. Beff et al., 2013; Whalley et al., 2017) and natural environments (e.g. root zone soil moisture, al Hagrey, 2007; Ain-Lhout et al., 2016).

To estimate the VSM (θ_w) from the electrical resistivity surveys, we used Archie's law. From Archie's law, we have:

$$\rho = \rho_w \Phi^m {S_w}^n \quad \text{(Equation 1)}$$

Here we use the parameters: ρ_w (pore water resistivity), ρ (bulk soil resistivity), Φ the water content, S_w the water saturation, n the porosity, and the parameter m which is an empirical fitting parameter. Using the generalised Archie's law (Shah and Singh, 2005; Glover, 2010), and assuming that the c parameter given by Shah and Singh (2005) = 1. This assumption was made as clay content in the soil was negligible (Sprenger et al. 2017), so the c parameter was likely to be around 1. Additionally, Shah and Singh (2005) suggest a high degree of uncertainty in c with low clay contents. We can also assume that m=n, which produces:

$$\rho = \rho_w (\Phi S_w)^m \quad \text{(Equation 2)}$$

240

241 And thus,

242 $$\rho = \rho_w(\theta_w)^m \quad \text{(Equation 3)}$$

243 This can then be re-arranged to give VSM (θ_w) (Equation 4).

244 $$\theta_w = \left(\frac{\rho_w}{\rho}\right)^{\frac{1}{m}} \quad \text{(Equation 4)}$$

245 Equation 4 includes the variables: In this study, the bulk resistivity is the inverted data from the
246 electrical resistivity tomography measurements (See section 3.2), and the pore water resistivity and
247 the m exponent were both estimated using field data (equations 2 and 3 respectively).

248 During the study period, there were infrequent measurements of the pore water resistivity, however,
249 after a large storm in January 2016, some measurements were taken at the forest site on the 8th
250 January from the upper 15 cm of the soil profile. Two samples were taken using MicroRhizon samplers
251 (Rhizosphere Research Products) and were analysed in the lab using a conductivity meter (Jenway
252 Model 4510). These measurements showed the average pore water resistivity to be 350 Ωm. We then
253 used this measured pore water resistivity (ρ_w) to calibrate m exponent, again by re-arranging the
254 generalised Archie's law to give Equation 5.

255 $$m = \frac{\log(\frac{\rho_w}{\rho})}{\log \theta_w} \quad \text{(Equation 5)}$$

256 The bulk resistivity (ρ_w) and VSM (θ_w) are the average measured resistivity and TDR measured soil
257 moisture over the 0 to 0.5 m depths, respectively. We assumed the pore water resistivity to be the
258 same at both sites, however, the bulk resistivity and the VSM differed between the heather and forest
259 site, and as such, site specific calibrations of the m exponent were carried out. At the heather site, the

260 average bulk resistivity was 820 Ωm and the average VSM 0.44 m^3 m^{-3}, which gave a m exponent of
261 1.04. At the forest site, the average bulk resistivity at 0.1-0.5 m depths was 790 Ωm and the average
262 VSM over that depth was 0.48 m^3 m^{-3}. This gave an m exponent of 1.10. These values were then used
263 as fixed parameters for all surveys, and are within the range of typical m exponents from the standard
264 Archie's law formulation (between 1.0 and 2.5) (Vereecken et al., 2006). Lower m exponents indicate
265 high connectivity of pore water. While the values estimated here might appear low, a study by Moreno
266 et al., (2015) found root zone m exponents of around 1.06 when the m exponent was estimated using
267 field data.

268 Equation 4 requires the pore water resistivity for every survey date. As this was only measured on the
269 8th January, we estimated it using Equation 6 (a further rearrangement of the generalized Archie's
270 law), which required: the m exponents calculated above; the average measured VSM (θ_w) at 0.1 and
271 0.5 m depths from the two TDR sensors at those depths; and the bulk resistivity (ρ) from each plot
272 survey at the same 0.1 or 0.5 m depths.

273 $$\rho_w = \rho {\theta_w}^m \quad \text{(Equation 6)}$$

274 The estimated pore water resistivities were mostly within the ranges of input waters (243-910 Ωm)
275 and drainage waters (164-500 Ωm), with variability linked to the movement of groundwater through
276 the profile at the flatter heather site and fast draining of input waters at the forest site due to the
277 rockier subsurface (Fig 3).

278 The VSM for each of the plot surveys was then calculated using Equation 4; with the calibrated
279 exponent (m) and the calibrated pore water resistivities (ρ_w) for each survey (as calculated above).
280 The VSM was interpolated from the resistivity data, and selected for 0.1 and 0.5 m depths, using the
281 surveyed bulk resistivity at those depths. The 0.1 and 0.5 m depths were chosen as they encompass
282 the whole typical root depth range of heather (*C. vulgaris*; 0.28 m) and Scots Pine (*P. sylvestris*; 0.48
283 m) (Jackson et al., 1996).

The method for estimating VSM for the 8.75 m transects was identical to that of the plots, including the same pore water resistivities and m exponent. Transect VSM was estimated from the surface to 0.5 m deep, with the depth limit of 0.5 m chosen because this depth encompassed the rooting zones of both heather and forest (Fig 4). The same depth limits were applied to the heather site for purposes of comparison.

Though the methods employed require TDR measured VSMs to estimate the ERT VSM, we tested both data sets for statistical differences using the Wilcoxon signed-rank test. This test was chosen as a non-parametric version of the paired t-test, and was required as both data sets are dependent. To assess the spatio-temporal variability of VSM, we calculated statistical variance across all of the surveys for both the heather and forest plots. This highlighted the areas in the plots where the soil moisture was more susceptible to change. To compliment this, and identify areas in the plots where there was pronounced wetting and drying, we calculated the spatio-temporal ranges of VSM. We then separated these into the variance and ranges for the growing (Mid-April to end of September) and non-growing season. The same methods employed for the plot surveys was also carried out on the 8.75 m transects for the full 0-0.5 m depth.

Correlations between the spatial patterns in temporal variability and ranges were then investigated with relation to the vegetation structure in the forest site using Spearman's correlation. Correlations between VSM and vegetation structure at the heather site were not carried out as the heather site was fairly uniform in canopy cover.

4. Results

4.1 Hydroclimate dynamics

306 During the study period, which ran from October 2015 to September 2016, there was 1334 mm
307 precipitation (Fig 5a), including a very wet December and early January which contributed 507 mm to
308 the overall total. Runoff during the period was 663 mm (though likely to be higher due to the
309 uncertainty surrounding the storm period) and 402 mm PET. Long term average air temperature
310 during the period was 6.8^{o}C. Along with the January storm, there were several hydrologically
311 interesting periods. Autumn 2015 was relatively dry, with lower than average rain fall. This was
312 followed by an exceptionally wet winter, with a large storm on 30th December, which caused
313 widespread flooding (Soulsby et al., 2017). Anomalously wet conditions persisted through January
314 2016. During this period, the regional precipitation total was 228% of the average winter precipitation
315 total. Subsequently, February was much drier. Spring 2016 was also relatively dry with only 84% of the
316 long-term average rainfall. The summer of 2016 was punctuated by large frontal precipitation events,
317 and was initially wet at the beginning, becoming drier towards the end, with particularly dry spells in
318 August and September (Fig 5a). The seasonal descriptions are from
319 http://www.metoffice.gov.uk/climate/uk/summaries.

320 Potential evapotranspiration over the period followed a seasonal cycle (Fig 5a), with low
321 evapotranspiration amounts (between 0-1 mm d^{-1}) and reduced variability in winter. Rates were
322 higher during the summer, with increased variability. The growing season's potential
323 evapotranspiration range was 4.4 mm per day (mean: 1.8mm), and the non-growing season range was
324 2.0 mm (mean: 0.4 mm). Evapotranspiration was around 70% of the precipitation input in the forest
325 site, and 55% of the total precipitation input in the heather site (Sprenger et al., 2017; Wang et al.,
326 2017).

327

328 **4.2 Volumetric soil moisture estimation at the plot sites.**

329 At the heather site, the average TDR measured VSM was 0.36 m^3 m^{-3}, with a standard deviation of
330 0.04 m^3 m^{-3} (Table 1). In comparison, the VSM estimated for the whole period using the ERT
331 measurements was 0.35 m^3 m^{-3} (Fig 5b). The wettest period for both the TDR and ERT VSM was the
332 January 2016 storm event. During the storm, the ERT-based VSM estimates were substantially higher
333 than the TDR VSM measurements (0.59 m^3 m^{-3} versus 0.42 m^3 m^{-3}, respectively). Apart from the storm
334 event, the interquartile range of ERT derived VSM in the heather plot was fairly constant. Overall, the
335 estimated VSM using the geophysics were generally consistent with the TDR measurements, and
336 captured the dynamics well (Fig 5b), with the Wilcoxon signed-rank test at the heather site showing
337 no statistical significant difference (p-value =<0.058). However, the forest site unsurprisingly did show
338 a significant difference (p-value =<0.01).

339 At the forest site, the average TDR measured VSM was 0.46 m^3 m^{-3}, with a standard deviation of 0.06
340 m^3 m^{-3} (Table 1). In comparison, the VSM estimated for the whole period from the ERT was 0.38 m^3
341 m^{-3} (Fig 5c). As in the heather site, the wettest period for both the TDR and ERT VSM was the January
342 storm event. Again, during that storm, the ERT VSM was higher than the TDR VSM (0.64 m^3 m^{-3} versus
343 0.55 m^3 m^{-3}, respectively). The estimated VSM using the geophysics exhibited a larger systematic shift
344 with TDR generated VSM time series than at the heather site, though still reproducing the ERT
345 dynamics well (Fig 5c)The interquartile ranges of the VSM in the forest plot was fairly heterogeneous,
346 with the VSM ranges largest during the wettest periods (Fig 5c).

347 Figures 6 and 7 show examples for wetting (17/11/15 – 08/01/16) and drying cycles (25/07/16 –
348 23/08/16) in the 3D ERT plots at 0.1 and 0.5 m. The dates were selected as they represented the
349 greatest wetting and drying during the study period, with 526 mm of rain during the wetting period,
350 and only 55 mm of precipitation during the period of drying. For the heather site at 0.1 m depth, there
351 was a zone of high VSM through the middle of the plot during all surveys. This expanded substantially
352 during the wetting period (Fig. 6a). During drying, VSM ranged from 0.2 to 0.6 m^3 m^{-3} on the 25/07/16
353 to a 0.2 to 0.5 m^3 m^{-3} on the 23/08/16 (Fig 7a). The western side, north east, and south east corners

of the plots were drier, with VSM ranging of 0.2-0.5 m^3 m^{-3} during both wetting (Fig 6a) and drying periods (Fig 7a) at 0.1 m. At 0.5 m, there was fairly similar VSM content between wetting (Fig 6b) and drying (Fig 7b), though after the January storm, VSM increased substantially.

At the forest site, VSM patterns during wetting and drying had a comparatively more heterogeneous pattern (Fig 6c and d; Fig 7c and d). The areas of highest mean VSM change were roughly correlated (Average correlation coefficient of 0.3, p-value <0.01) with the areas of reduced canopy cover, with the areas of greatest change during drying being around trees (Fig 7c). This is especially clear with the tree at 2 x 5.5 m. The VSM at 0.1 m increased during wetting, ranging from 0.2 to 0.7 m^3 m^{-3} on 17/11/15 to 0.2 to 0.8 m^3 m^{-3} on the 08/01/16 (Fig 6c). During the drying period, there was general drying across the whole plot at 0.1 m (Fig 7c). Unlike the heather plot, at 0.5 m depths there was a slight increase in VSM (Fig 7d). This was probably due to wetting fronts moving down through the profile from early August rain.

4.3 Spatio-temporal heterogeneity in plot volumetric VSM

At the heather site (Fig 8a), the statistical variance of the ERT VSM showed contrasts, with variances ranging from 0 to 0.01 $(m^3\ m^{-3})^2$. With the area of highest variability roughly correlating (r= 0.45, p-value = <0.01) with the wettest locations in the plot (Fig 6a, 7a, and 8a). In the forest site, the temporal variance in the spatial domain volumetric VSM was more homogeneous than at heather site (Fig 8a versus 8b), ranging from 0 to 0.005 $(m^3\ m^{-3})^2$ (Fig 8b), with the most variable areas in the spatial domain mostly located near trees in the north and east areas of the plot (c.f. Fig 2). Ranges of soil moisture were larger at the heather site (Fig 8a), with the highest ranges also centred on the wettest parts of the plot. Ranges of around 0.2 m^3 m^{-3} were located near the trees at the forest site, with the smallest ranges located at the south-west corner of the plot in the area with least canopy cover (Fig 8b).

The variance VSM was then investigated for the growing (Mid-April to end of September) and non-growing season at the 0.1 m depth slices from the plot surveys (Fig 9). At the heather site (Fig 9a), there were striking differences in the patterns of VSM during both seasons. During the growing season, the spatial variance in VSM temporal changes were low, with variance between 0 and 0.001 $(m^3\ m^{-3})^2$. In the non-growing season VSM variance was much more variable and higher (ranging from 0.002 to 0.01 $(m^3\ m^{-3})^2$). At the forest site (Fig 9b), spatial patterns of VSM temporal variance were much more homogeneous than the heather site, spanning a range of 0 – 0.005 $(m^3\ m^{-3})^2$in both seasons. There were however subtle differences between the non-growing and growing seasons, with the growing season having the higher variance in VSM, and in particular. The variances were highest in areas where there were trees.

4.4 Using high spatial resolution transect measurements to investigate root zone soil moisture

The transect in the forest was sited to encompass the root zone extent of two established Scots Pine trees. The transect data showed again that at the heather site, VSM variances were mostly low at all depths, though there were some VSM variances of 0.01 $(m^3\ m^{-3})^2$ close to the surface (>0.3 m deep) (Fig 10a). The ranges of VSM also fairly low, mostly 0 - 0.2 $m^3\ m^{-3}$, but with some ranges of 0.3 to 0.5 $m^3\ m^{-3}$. In both plots of VSM variance and range, there was a defined boundary at 0.25 - 0.3 m where variance and range in VSM decreased substantially (Fig 11a). At the forest site, the VSM variance ranged from 0 to 0.01 $(m^3\ m^{-3})^2$, and was generally much more heterogeneous than the heather site (Fig 10b), as a consequence of the high resistivity scree underlying the forest site (see also Fig 4). As shown for the plots in Figures 8 and 9, the greatest heterogeneity in variance and range of VSM occurred during the growing season at the forest site, with VSM ranges in upper 0.5 m of 0.1 to 0.5 $m^3\ m^{-3}$; Fig 11b). After 0.50 m, the range generally decreased to 0 to 0.15 $m^3\ m^{-3}$. Overall, the greatest

variability with depth occurred within the root zone and was centred around the two trees (Fig 10b and Fig 11b).

5. Discussion

5.1 Estimating plot scale soil moisture from repeat plot scale ERT measurements

The approach of using plot scale ERT measurements to estimate soil moisture was able to capture the temporal patterns in VSM dynamics such as drying and wetting, at both sites, though the degree of change differed between sites. Though this could have been linked to the electrical properties of the thin peat layer at both sites, the soils at both studies sites are minerogenic, with much of the organic horizon comprising of litter. As such, the differences in the electrical properties of the thin peat layer are likely unimportant when you take into account the greater depth of minerogenic material. It is more likely, that this difference in correspondence between the ERT VSM and the TDR VSM between the heather and forest site is linked either to: (a) the greater subsurface heterogeneity at the forest site caused by the tree roots and much rockier sub-soil influencing the soil physical properties, which leads to higher heterogeneity in the resistivity of the subsurface. Or, (b) preferential flow paths which are very common in forest soils (Sidle et al., 2001), and influence the ERT results, but are not picked up by the point TDR measurements. Something also found by Hubner et al. (2015). It could also be linked to the sampling occasions of the ERT surveys integrating the larger scale heterogeneity of the subsurface (something which not possible when using point measurements) (Hübner et al., 2015), and the choice of electrode spacing (Rey et al., 2006), which was driven by the site characteristics. Heterogeneity in the subsurface can be in the form of tree roots, airspaces between rocks in the subsurface (Calamita et al., 2015), both of which are known to be present at the forest site. However, the generally reasonable correspondence between ERT and the TDR VSM time series (especially in the heather site) adds confidence to the usefulness of using ERT in the spatial estimation of VSM for plots

425 scale studies. Though the temporal comparison of ERT VSM to TDR VSM was poorer at the forest site,
426 the temporal dynamics of VSM from both methods was captured, with the same flashy VSM response
427 to large precipitation inputs.

428 Using ERT to survey plot scale resistivity and estimation of VSM facilitates the enhanced collection of
429 large spatial datasets, its visualisation, analysis and interpretation in contrast to long term point
430 measured VSM time series (Brunet et al., 2010). This is important as it allows the synoptic visualisation
431 of spatial patterns and temporal dynamics of VSM (Jayawickreme et al., 2008), something especially
432 useful when comparing VSM under different vegetation types, where heterogeneity in vegetation
433 structure might have a strong influence on VSM (D'Odorico et al., 2007).

434 During the January 2016 storm, both sites exhibited a poorer correspondence of the geophysically
435 derived VSM with the TDR measured VSM. This is potentially linked to a change in soil water chemistry
436 during the large events, something already documented in the Scottish Highlands (e.g. Jenkins 1989).
437 The extreme volume of rainfall instigated a change in water conductivity, with the increased influence
438 of low conductivity rainfall replacing the soil water leading to an increase of resistivity with wetness
439 (Chambers et al., 2014; Mueller et al., 2016). The use of the measured natural water conductivity in
440 the catchment alongside the estimation of the pore water resistivity allowed us to account for this. It
441 is also likely that the TDR VSM was influenced by the change in conductivity during the storm period
442 as TDR methods are also susceptible to conductivity changes (see Topp et al., 1994). As such, this
443 suggests that the assumption of stable soil water resistivity over time may not always hold at this site
444 (Brunet et al., 2010). For a reasonable estimation of VSM time variable conductivities need to be
445 addressed, as carried out in this study by using TDR and ERT measurements to estimate the soil water
446 conductivity. The storm period and the consequent drying highlight some of the limits of the approach
447 used in this study, such as the absence of a soil water conductivity time series is ideally needed to
448 increase the accuracy of estimated VSM, especially during highly variable hydrometer logical
449 conditions. Specifically, the lack of year-long soil water resistivity measurements required their

estimation using the TDR data. This effectively meant that the TDR data was used to estimate the soil water conductivity and the m exponent, leading to interdependence of the ERT and TDR VSM time series making statistical comparison challenging. Though based on empirical data, the uncertainty surrounding the estimation of the m exponent could also have been improved through the inclusion of more periods in which ERT and soil water measurement data overlapped. However, this was not possible during this study. For future studies, soil water resistivity measurements concurrent to the ERT surveys would be recommended.

Importantly though, the use of both 2D (transects) and 3D (plot) measurements has distinct advantages for surveying the subsurface as this allows high resolution, non-destructive (i.e. repeatable) visualisation of water distribution (Séger et al., 2009). The benefits of using plot measurements are that they allow the characterization of subsurface spatial heterogeneity in terms of location and extent, something not possible with transect measurements as the spatial patterns may not be orientated with the transect axis (Bentley and Gharibi 2004). In turn, transect measurements are the most widely applied ERT method and can be set up and surveyed quickly (Loke et al., 2013), with the major benefit of being able to rapidly extend the survey distances using "roll-along" methods (Donohue et al., 2012). We therefore integrated insights from both sampling approaches, overcoming the issues of low resolution due to electrode spacing in the plots, and avoiding the chance of missing subsurface spatial heterogeneity by only using transects.

As explained in section 3.3, using Archie's law requires either provision of data for, or estimation of, the parameters and certain variables (Singha and Gorelick, 2006). This estimation introduces significant uncertainty into the analysis (Brunet et al., 2010), and must be constrained through either laboratory (Brunet et al., 2010), or field data estimation (Moreno et al., 2015) as done here. In this study, we used the generalised form of Archie's law (Glover, 2010) for which the variables required to

474 estimate VSM are bulk resistivity, pore water resistivity and the m exponent. Though calibration of
475 the m expoenent is not required as values have been previously published for many substrates
476 (Friedman, 2005; Vereecken et al., 2006), calibrating the factor based on site specific field data usually
477 produces a much more realistic value (Moreno et al., 2015). Specifically, the m exponent is an
478 empirical coefficient which relates porosity to the conductivity of the substrate (Friedman, 2005),
479 typically ranging from 1.0 to 2.5 (Vereecken et al., 2006). In our study, both sites were between 1.0
480 and 1.1. Our low values are likely due to the high sand content in our soils (Sprenger et al., 2017), and
481 the fact that we employed field calibration rather than the usual lab calibration, which - due to its
482 destructive nature - may have changed the structure of the soil leading to the higher estimates due to
483 compaction and decrease in permeability of the soil core (Moreno et al., 2015).

484

485

486 **5.2 Differences in spatio-temporal dynamics of soil moisture between heather and forest dominated**
487 **vegetation assemblages**

488 The heather site showed low temporal (mostly seasonal) variability in both the TDR and average ERT
489 VSM. In comparison, the forest site showed a higher, more marked temporally variable VSM response
490 to precipitation inputs. Higher VSMs in the forest site can be attributed to higher organic content of
491 soils (Jamison and Kroth, 1958; Sprenger et al., 2017). The larger temporal variability during the
492 growing season at the forest site can be linked to the influence of vegetation when interception and
493 evapotranspiration losses were higher (Ain-Lhout et al., 2016); and the greater subsurface drainage at
494 this site (Geris et al., 2015). Subsurface drainage explains the flashy soil moisture response, which is
495 likely linked to the coarse scree freely draining material underlying the forest site with its high porosity.

496 While temporal variability in the TDR and ERT VSM data highlighted differences and potential
497 vegetation influences at both sites, the most marked differences were apparent when comparing the

498 plots. Spatial variability of VSM in the heather site was lower than the forest site during periods of
499 drying and wetting. That is, the VSM pattern remained relatively uniform during both the wet up and
500 drying periods. This can be linked to the more uniform canopy (Soulsby et al., 2017), which is
501 supported by the lack of variation in mean soil moisture change and higher net precipitation. The
502 patterns of soil moisture were closely correlated with the areas of higher VSM variance, which is likely
503 associated with the relationship of VSM, subsurface structure, and soil physical properties (Cosby et
504 al., 1984; Qu et al., 2014). Future work will test this hypothesis further.

505 The relationship between VSM and areas of highest variability in VSM was more complex at the forest
506 site, with non-uniform wetting and drying. This is most likely linked to external factors out with the
507 subsurface structure, for example, the heterogeneity in canopy cover, patterns of throughfall and
508 stemflow inputs (Buttle et al., 2014; Ma et al., 2014), the less dense vegetation canopy, and a different
509 sub-canopy microclimate (Oren and Pataki, 2001; Lin, 2010). Work comparing spatial soil moisture
510 patterns under forest and shrub vegetation is sparse in temperate settings, with most research carried
511 out in semi-arid regions based mostly on point soil moisture measurements (e.g. Breshears et al.,
512 1999). ERT has been successfully employed in comparing vegetation types; for example, Jayawickreme
513 et al., (2008) conducted a study on the differences between forest and grass land using 2D transects.
514 They found that forest exerted a stronger control on VSM than the grassland, as was the case with the
515 forest site in our study. Here, reduced canopy cover and the mean change of VSM were roughly
516 correlated (Correlation coefficient of 0.3, p-value = <0.01), with a potential link to the presence of, or
517 rather distance from trees (e.g. Elliott et al., 1998). This link to the vegetation became even clearer in
518 the VSM range, where the areas of largest VSM ranges corresponded to the trees and were related to
519 the highest root density near the tree trunk (Elliott et al., 1998; al Hagrey, 2007) and the distributed
520 point source inputs of large volumes of water through stem flow (Liang et al., 2011; Jian et al., 2014).

521 Comparing the growing and non-growing season mean soil moisture changes at the heather and forest
522 sites highlighted further differences. The heather plot showed little spatial change in temporal VSM

variability across the whole plot during the growing season whereas the forest was more heterogeneous, with areas of much greater VSM temporal variance near the bole of the trees. This is likely linked to the water partitioning and water use by the trees. The smaller VSM temporal variance seen at the heather plot was most likely again attributable to the subsurface structure and a likely greater variability in soil properties (though not specifically investigated) (Cosby et al., 1984; Qu et al., 2014). The low overall change, despite larger amounts of precipitation available for infiltration, highlights the link of VSM to the (more homogenous) vegetation cover, water use and deeper drainage. Wang et al., (2017), found the transpiration of heather to be around 17% less than the forest. This would impose a more marked vegetation influence on soil moisture at the forest site during drier periods (Warren, 2015). Soulsby et al. (2017) found that low intensity rainfall events had greater percentage interception losses than the larger events in the Bruntland Burn, a finding corroborated elsewhere by (Toba and Ohta, 2005). Higher VSM variance and range during the non-growing season at the heather site when compared to the forest site reflect the larger volume of precipitation inputs and subsequent drying/drainage, with a pattern that is closely linked to the aforementioned subsurface structure at the heather site. The cause for reduced variance and range in VSM at the forest site during the non-growing season could be due to the greater drainage, and distribution of water by the canopy during the period.

The surveying of transects with small electrode spacing under both the heather and forest vegetation sites during the growing season elucidated some of the findings from the 3D plot studies. The VSM variability between the transect surveys showed that both sites underwent changes in VSM (translatable to overall drying during this period). The drying at the heather site was confined to the upper 0.2 m, which corresponds to the rooting depths of heather (95% of roots are within the upper 0.2 m) (Sprenger et al., 2017). In the forest site, drying was focussed around the two individual trees and extended to 0.5 m deep, again corresponding to the likely maximum rooting depth of Scots Pine (Haria and Price, 2000). The presence of clear drying in the high resolution transects supports the

548 inference that vegetation exerts a control on soil moisture at both sites. At the heather site (due to
549 the higher number of individual plants), the vegetation exerts a control on spatial soil moisture
550 patterns due to more homogenous canopy and more homogenous distribution of water. This finding
551 is corroborated by Canton et al. (2004) whom looked at the relationship between canopy openness
552 and soil moisture variability.

553 The presented data has highlighted differences in the interactions of heather and forest vegetation
554 with soil moisture, which has implications for both land use and climate change. In Scotland, these
555 findings are highly relevant as there are currently ongoing plans to afforest large areas of land
556 (https://www.gov.uk/government/publications/2010-to-2015-government-policy-forests-and-
557 woodland/2010-to-2015-government-policy-forests-and-woodland), and specifically, in the
558 Cairngorm National Park of which the Bruntland Burn is part (http://cairngorms.co.uk/working-
559 partnership/consultations/thebig9). This potential widespread vegetation change might change the
560 water balance within the landscape (Geris et al., 2015), through an increase in forest leading to higher
561 evapotranspirative losses and water deficits during the growing season. This finding is corroborated
562 by Haria and Price (2000), whom found that ET was over 40% greater in a forest site. These changes
563 would have significant bearing on hydrological stores and flows. Additionally, the projected shift of
564 precipitation away from summer to the winter period (UKCP 09) has the potential to alter the
565 feedbacks between soil moisture and vegetation water use, increasing growing season soil moisture
566 deficits (Capell et al., 2013), given that the strongest influence vegetation has over soil moisture is
567 during the growing season, where less precipitation will increase soil moisture deficits. Thus, our study
568 has shown the potential heterogeneity in water sources in the soil could be subject to both major and
569 subtle changes as a result of widespread increases in forest cover through more intensive water use,
570 something further heightened through the potential decrease in growing season precipitation.

571

6. Conclusion

This work has highlighted the difference in soil moisture variability under two contrasting vegetation types, and showed the value of using ERT geophysics to help understand the influence of vegetation on VSM dynamics and patterns. The use of mixed ERT approaches (e.g. 3D and 2D surveys) helped to visualise and quantify vegetation-soil water interactions, and enabled the investigation of these interactions at different spatial scales and resolutions, something which would have been not possible using point measurements alone. The presented plot measurements allowed high resolution analysis of VSM spatially, and captured the heterogeneity associated with vegetation distribution as well as temporal dynamics. In addition, the transect measurements allowed a high-resolution analysis of effects of vegetation on VSM within the root zone.

Acknowledgements

We thank the British Atmospheric Data Centre for the provision of meteorological data. We also thank the European Research Council ERC (project GA 335910 VEWA) for funding through the VeWa project and the Leverhulme Trust for funding through PLATO (RPG-2014-016). The authors are grateful to the editorial comments of Daniele Penna and careful constructive criticism from three anonymous reviewers which help improve the paper.

590 **References**

591 '2010 to 2015 Government Policy: Forests and Woodland - GOV.UK'. 2017. May 5.
592 https://www.gov.uk/government/publications/2010-to-2015-government-policy-forests-
593 and-woodland/2010-to-2015-government-policy-forests-and-woodland.

594 Ain-Lhout, F., S. Boutaleb, M. C. Diaz-Barradas, J. Jauregui, and M. Zunzunegui. 2016. 'Monitoring the
595 Evolution of Soil Moisture in Root Zone System of Argania Spinosa Using Electrical Resistivity
596 Imaging'. *Agricultural Water Management* 164: 158–166.

597 Archie, G.E. 1942. 'The Electrical Resistivity Log as an Aid in Determining Some Reservoir
598 Characteristics'. *Transactions of the AIME* 146 (1): 54–62. doi:10.2118/942054-G.

599 Beff, L, T Günther, B Vandoorne, V Couvreur, and M Javaux. 2013. 'Three-Dimensional Monitoring of
600 Soil Water Content in a Maize Field Using Electrical Resistivity Tomography'. *Hydrology and*
601 *Earth System Sciences* 17 (2): 595–609.

602 Bentley, L.R., and M Gharibi. 2004. 'Two-and Three-Dimensional Electrical Resistivity Imaging at a
603 Heterogeneous Remediation Site'. *Geophysics* 69 (3): 674–680.

604 Besson, A, I. Cousin, A. Dorigny, M. Dabas, and Dominique King. 2008. 'The Temperature Correction
605 for the Electrical Resistivity Measurements in Undisturbed Soil Samples: Analysis of the
606 Existing Conversion Models and Proposal of a New Model'. *Soil Science* 173 (10): 707–720.

607 Binley, A., S.S. Hubbard, J.A. Huisman, A. Revil, D.A. Robinson, K. Singha, and L.D. Slater.
608 "The Emergence of Hydrogeophysics for Improved Understanding of Subsurface
609 Processes over Multiple Scales." *Water Resources Research* 51, no. 6 (2015): 3837–
610 3866.

611 Birkel, C., D. Tetzlaff, S. M. Dunn, and C. Soulsby. 2010. 'Towards a Simple Dynamic Process
612 Conceptualization in Rainfall–runoff Models Using Multi-Criteria Calibration and Tracers in

613 Temperate, Upland Catchments'. *Hydrological Processes* 24 (3): 260–275.
614 doi:10.1002/hyp.7478.

615 Boaga, J., M. Rossi, and G. Cassiani. "Monitoring Soil-Plant Interactions in an Apple Orchard Using 3D
616 Electrical Resistivity Tomography." *Procedia Environmental Sciences*, Four Decades of
617 Progress in Monitoring and Modeling of Processes in the Soil-Plant-Atmosphere System:
618 Applications and Challenges, 19 (January 1, 2013): 394–402.
619 doi:10.1016/j.proenv.2013.06.045.

620 Breshears, D.D., and F.J. Barnes. 1999. 'Interrelationships between Plant Functional Types and Soil
621 Moisture Heterogeneity for Semiarid Landscapes within the Grassland/forest Continuum: A
622 Unified Conceptual Model'. *Landscape Ecology* 14 (5): 465–478.

623 Brillante, L., O. Mathieu, B. Bois, C. van Leeuwen, and J. Lévêque. 2015. 'The Use of Soil Electrical
624 Resistivity to Monitor Plant and Soil Water Relationships in Vineyards'. *SOIL* 1 (1): 273–286.

625 Brocca, L., T. Tullo, F. Melone, T. Moramarco, and R. Morbidelli. 2012. 'Catchment Scale Soil
626 Moisture Spatial–temporal Variability'. *Journal of Hydrology* 422–423 (February): 63–75.
627 doi:10.1016/j.jhydrol.2011.12.039.

628 Brunet, P, R Clément, and C Bouvier. 2010. 'Monitoring Soil Water Content and Deficit Using
629 Electrical Resistivity Tomography (ERT) – A Case Study in the Cevennes Area, France'. *Journal*
630 *of Hydrology* 380 (1–2): 146–53. doi:10.1016/j.jhydrol.2009.10.032.

631 Buttle, J.M., H.J. Toye, W.J. Greenwood, and R. Bialkowski. 2014. 'Stemflow and Soil Water Recharge
632 during Rainfall in a Red Pine Chronosequence on the Oak Ridges Moraine, Southern Ontario,
633 Canada'. *Journal of Hydrology* 517 (September): 777–90. doi:10.1016/j.jhydrol.2014.06.014.

634 Calamita, G., A. Perrone, L. Brocca, B. Onorati, and S. Manfreda. 2015. 'Field Test of a Multi-
635 Frequency Electromagnetic Induction Sensor for Soil Moisture Monitoring in Southern Italy

636 Test Sites'. *Journal of Hydrology* 529 (October):316–29.
637 https://doi.org/10.1016/j.jhydrol.2015.07.023.
638
639 Cantón, Y., A. Solé-Benet, and F. Domingo. 2004. 'Temporal and Spatial Patterns of Soil Moisture in
640 Semiarid Badlands of SE Spain'. *Journal of Hydrology* 285 (1): 199–214.
641 doi:10.1016/j.jhydrol.2003.08.018.

642 Capell, R., D. Tetzlaff, and C. Soulsby. 2013. 'Will Catchment Characteristics Moderate the Projected
643 Effects of Climate Change on Flow Regimes in the Scottish Highlands?: Effects of climate
644 change in catchments along a hydroclimate transect'. *Hydrological Processes* 27 (5): 687–99.
645 doi:10.1002/hyp.9626.

646 Chambers, J.E., D.A. Gunn, P.B. Wilkinson, P.I. Meldrum, E. Haslam, S. Holyoake, M. Kirkham, O.
647 Kuras, A. Merritt, and J. Wragg. 2014. '4D Electrical Resistivity Tomography Monitoring of
648 Soil Moisture Dynamics in an Operational Railway Embankment'. *Near Surface Geophysics* 12
649 (2007). doi:10.3997/1873-0604.2013002.

650 Chambers, J., R. Ogilvy, O. Kuras, J. Cripps, and P. Meldrum. "3D Electrical Imaging of Known Targets
651 at a Controlled Environmental Test Site." *Environmental Geology* 41, no. 6 (February 1,
652 2002): 690–704. doi:10.1007/s00254-001-0452-4.
653 Coenders-Gerrits, A. M. J., L. Hopp, H. H. G. Savenije, and L. Pfister. 2013. 'The Effect of Spatial
654 Throughfall Patterns on Soil Moisture Patterns at the Hillslope Scale'. *Hydrol. Earth Syst. Sci*
655 17: 1749–1763.

656 Cosby, B. J., G. M. Hornberger, R. B. Clapp, and ToR Ginn. 1984. 'A Statistical Exploration of the
657 Relationships of Soil Moisture Characteristics to the Physical Properties of Soils'. *Water*
658 *Resources Research* 20 (6): 682–690.

659 Cosh, M.H., T.J. Jackson, R. Bindlish, and J.H. Prueger. 2004. 'Watershed Scale Temporal and Spatial
660 Stability of Soil Moisture and Its Role in Validating Satellite Estimates'. *Remote Sensing of*
661 *Environment* 92 (4): 427–35. doi:10.1016/j.rse.2004.02.016.

662 Dick, J. J., D. Tetzlaff, C. Birkel, and C. Soulsby. 2014. 'Modelling Landscape Controls on Dissolved
663 Organic Carbon Sources and Fluxes to Streams'. *Biogeochemistry*, December, 1–14.

664 D'Odorico, P, K. Caylor, G.S. Okin, and T.M. Scanlon. 2007. 'On Soil Moisture-Vegetation Feedbacks
665 and Their Possible Effects on the Dynamics of Dryland Ecosystems: SOIL MOISTURE-
666 Vegetation Feedbacks'. *Journal of Geophysical Research: Biogeosciences* 112 (G4): n/a-n/a.
667 doi:10.1029/2006JG000379.

668 Donohue, S, M. Long, P. O'Connor, and others. 2012. 'Multi-Method Geophysical Mapping of Quick
669 Clay'. http://researchrepository.ucd.ie/handle/10197/4891.

670 Dunn, S. M., and R. Mackay. "Spatial Variation in Evapotranspiration and the Influence of Land Use
671 on Catchment Hydrology." *Journal of Hydrology* 171, no. 1 (September 1, 1995): 49–73.
672 doi:10.1016/0022-1694(95)02733-6.

673 Elliott, J. A., B. M. Toth, R. J. Granger, and J. W. Pomeroy. 1998. 'Soil Moisture Storage in Mature and
674 Replanted Sub-Humid Boreal Forest Stands'. *Canadian Journal of Soil Science* 78 (1): 17–27.
675 doi:10.4141/S97-021.

676 Entekhabi, D, I. Rodriguez-Iturbe, and F. Castelli. 1996. 'Mutual Interaction of Soil Moisture State and
677 Atmospheric Processes'. *Journal of Hydrology* 184 (1–2): 3–17.

678 Ford, E. D., and J. D. Deans. 1978. 'The Effects of Canopy Structure on Stemflow, Throughfall and
679 Interception Loss in a Young Sitka Spruce Plantation'. *Journal of Applied Ecology*, 905–917.

680 Friedman, S.P. 2005. 'Soil Properties Influencing Apparent Electrical Conductivity: A Review'.
681 *Computers and Electronics in Agriculture*, Applications of Apparent Soil Electrical
682 Conductivity in Precision Agriculture, 46 (1–3): 45–70. doi:10.1016/j.compag.2004.11.001.

683 Garré, S., M. Javaux, J. Vanderborght, L. Pagès, and H. Vereecken. "Three-Dimensional Electrical
684 Resistivity Tomography to Monitor Root Zone Water Dynamics." *Vadose Zone Journal* 10, no.
685 1 (February 1, 2011): 412–24. doi:10.2136/vzj2010.0079.

686 Geris, J, D. Tetzlaff, J. McDonnell, and C. Soulsby. 2015. 'The Relative Role of Soil Type and Tree
687 Cover on Water Storage and Transmission in Northern Headwater Catchments: soil and
688 vegetation effects on water storage and transmission'. *Hydrological Processes* 29 (7): 1844–
689 60. doi:10.1002/hyp.10289.

690 Geris, J., D. Tetzlaff, and C. Soulsby. 2015. 'Resistance and Resilience to Droughts: Hydropedological
691 Controls on Catchment Storage and Run-off Response: Hydropedological Controls on
692 Drought Resistance and Resilience'. *Hydrological Processes* 29 (21): 4579–93.
693 doi:10.1002/hyp.10480.

694 Glover, Paul W. J. 2010. 'A Generalized Archie's Law for N Phases'. *GEOPHYSICS* 75 (6): E247–65.
695 doi:10.1190/1.3509781.

696 Hagrey, S.A. al. 2007. 'Geophysical Imaging of Root-Zone, Trunk, and Moisture Heterogeneity'.
697 *Journal of Experimental Botany* 58 (4): 839–854.

698 Haria, A.H., and D.J. Price. 2000. 'Evaporation from Scots Pine (Pinus Sylvestris) Following Natural Re-
699 Colonisation of the Cairngorm Mountains, Scotland'. *Hydrology and Earth System Sciences*
700 *Discussions* 4 (3): 451–461.

701 Hasselquist, N.J., M.F. Allen, and L.S. Santiago. 2010. 'Water Relations of Evergreen and Drought-
702 Deciduous Trees along a Seasonally Dry Tropical Forest Chronosequence'. *Oecologia* 164 (4):
703 881–90. doi:10.1007/s00442-010-1725-y.

704 Helvey, J, and J.H. Patric. 1965. 'Canopy and Litter Interception of Rainfall by Hardwoods of Eastern
705 United States'. *Water Resources Research* 1 (2): 193–206.

706 Hübner, R., K. Heller, T. Günther, and A. Kleber. "Monitoring Hillslope Moisture Dynamics with
707 Surface ERT for Enhancing Spatial Significance of Hydrometric Point Measurements."
708 *Hydrology and Earth System Sciences* 19, no. 1 (2015): 225.

709 Jackson, R. B., J. Canadell, James R. Ehleringer, H. A. Mooney, O. E. Sala, and E. D. Schulze. 1996. 'A
710 Global Analysis of Root Distributions for Terrestrial Biomes'. *Oecologia* 108 (3): 389–411.

711 Jamison, V. C., and E. M. Kroth. 1958. 'Available Moisture Storage Capacity in Relation to Textural
712 Composition and Organic Matter Content of Several Missouri Soils'. *Soil Science Society of*
713 *America Journal* 22 (3): 189–192.

714 Jayawickreme, D.H., R.L. Van Dam, and D.W. Hyndman. 2008. 'Subsurface Imaging of Vegetation,
715 Climate, and Root-Zone Moisture Interactions'. *Geophysical Research Letters* 35 (18).
716 doi:10.1029/2008GL034690.

717 Jenkins, A. 1989. 'Storm Period Hydrochemical Response in an Unforested Scottish Catchment'.
718 *Hydrological Sciences Journal* 34 (4): 393–404.

719 Jian, S.Q, C. Zhao, S. Fang, and Kai Yu. 2014. 'Characteristics of Caragana Korshinskii and Hippophae
720 Rhamnoides Stemflow and Their Significance in Soil Moisture Enhancement in Loess Plateau,
721 China'. *Journal of Arid Land* 6 (1): 105–116.

722 Liang, W, K.I. Kosugi, and T. Mizuyama. 2011. 'Soil Water Dynamics around a Tree on a Hillslope with
723 or without Rainwater Supplied by Stemflow: soil water dynamics with or without stemflow'.
724 *Water Resources Research* 47 (2): n/a-n/a. doi:10.1029/2010WR009856.

725 Lin, B.B. 2010. 'The Role of Agroforestry in Reducing Water Loss through Soil Evaporation and Crop
726 Transpiration in Coffee Agroecosystems'. *Agricultural and Forest Meteorology* 150 (4): 510–
727 518.

728 Loke, M.H., J.E. Chambers, D.F. Rucker, O. Kuras, and P.B. Wilkinson. 2013. 'Recent Developments in
729 the Direct-Current Geoelectrical Imaging Method'. *Journal of Applied Geophysics* 95
730 (August): 135–56. doi:10.1016/j.jappgeo.2013.02.017.

731 Ma, R, A. McBratney, B. Whelan, B. Minasny, and M. Short. 2011. 'Comparing Temperature
732 Correction Models for Soil Electrical Conductivity Measurement'. *Precision Agriculture* 12 (1):
733 55–66.

734 Ma, Y, R.L. Van Dam, and D.H. Jayawickreme. 2014. 'Soil Moisture Variability in a Temperate
735 Deciduous Forest: Insights from Electrical Resistivity and Throughfall Data'. *Environmental*
736 *Earth Sciences* 72 (5): 1367–81. doi:10.1007/s12665-014-3362-y.

737 Mittelbach, Heidi, Irene Lehner, and Sonia I. Seneviratne. 2012. 'Comparison of Four Soil Moisture
738 Sensor Types under Field Conditions in Switzerland'. *Journal of Hydrology* 430–431 (April):
739 39–49. doi:10.1016/j.jhydrol.2012.01.041.

740 Moreno, Z, A. Arnon-Zur, and A. Furman. 2015. 'Hydro-Geophysical Monitoring of Orchard Root
741 Zone Dynamics in Semi-Arid Region'. *Irrigation Science* 33 (4): 303–18. doi:10.1007/s00271-
742 015-0467-3.

743 Mueller, M.H., A. Alaoui, and C. Alewell. 2016. 'Water and Solute Dynamics during Rainfall Events in
744 Headwater Catchments in the Central Swiss Alps under the Influence of Green Alder Shrubs
745 and Wetland Soils: Water and Solute Dynamics During Rainfall in Headwater Catchments'.
746 *Ecohydrology* 9 (6): 950–63. doi:10.1002/eco.1692.

747 Murphy et al., 2009. 'UK Climate Projections Science Report: Climate Change Projections'. Exeter:
748 Met Office Hadley Centre.

749 'National Park Partnership Plan 2017-2022: Consultation - Cairngorms National Park
750 AuthorityCairngorms National Park Authority'. 2017. May 5.
751 http://cairngorms.co.uk/working-partnership/consultations/thebig9/.

752 Oren, R, and D.E. Pataki. 2001. 'Transpiration in Response to Variation in Microclimate and Soil
753 Moisture in Southeastern Deciduous Forests'. *Oecologia* 127 (4): 549–559.

754 Peterson, A.M., W.D. Helgason, and A.M. Ireson. 2016. 'Estimating Field-Scale Root Zone Soil
755 Moisture Using the Cosmic-Ray Neutron Probe'. *Hydrology and Earth System Sciences* 20 (4):
756 1373–85. doi:10.5194/hess-20-1373-2016.

757 Porporato, A, E. Daly, and I. Rodriguez-Iturbe. 2004. 'Soil Water Balance and Ecosystem Response to
758 Climate Change'. *The American Naturalist* 164 (5): 625–32. doi:10.1086/424970.

759 Pypker, T.G., B.J. Bond, T.E. Link, D. Marks, and M.H. Unsworth. 2005. 'The Importance of Canopy
760 Structure in Controlling the Interception Loss of Rainfall: Examples from a Young and an Old-
761 Growth Douglas-Fir Forest'. *Agricultural and Forest Meteorology* 130 (1): 113–129.

762 Qu, W., H. R. Bogena, J. A. Huisman, G. Martinez, Y. A. Pachepsky, and H. Vereecken. 2014. 'Effects
763 of Soil Hydraulic Properties on the Spatial Variability of Soil Water Content: Evidence from
764 Sensor Network Data and Inverse Modeling'. *Vadose Zone Journal* 13 (12): 0.
765 doi:10.2136/vzj2014.07.0099.

766 Rey, E, D. Jongmans, P. Gotteland, and S. Garambois. 2006. 'Characterisation of Soils with Stony
767 Inclusions Using Geoelectrical Measurements'. *Journal of Applied Geophysics* 58 (3): 188–
768 201. doi:10.1016/j.jappgeo.2005.06.003.

769 Reyer, C.P.O., S. Leuzinger, A. Rammig, Annett Wolf, Ruud P. Bartholomeus, Antonello Bonfante,
770 Francesca de Lorenzi, et al., 2013. 'A Plant's Perspective of Extremes: Terrestrial Plant
771 Responses to Changing Climatic Variability'. *Global Change Biology* 19 (1): 75–89.
772 doi:10.1111/gcb.12023.

773 Rigling, A, C. Bigler, B. Eilmann, E. Feldmeyer-Christe, U. Gimmi, C. Ginzler, U. Graf, et al., 2013.
774 'Driving Factors of a Vegetation Shift from Scots Pine to Pubescent Oak in Dry Alpine
775 Forests'. *Global Change Biology* 19 (1): 229–40. doi:10.1111/gcb.12038.

776 Robinson, D. A., A. Binley, N. Crook, F. D. Day-Lewis, T. P. A. Ferré, V. J. S. Grauch, R. Knight, et al.,
777 2008. 'Advancing Process-Based Watershed Hydrological Research Using near-Surface
778 Geophysics: A Vision For, and Review Of, Electrical and Magnetic Geophysical Methods'.
779 *Hydrological Processes* 22 (August): 3604–35. doi:10.1002/hyp.6963.

780 Rodriguez-Iturbe, I., P. D'Odorico, A. Porporato, and L. Ridolfi. 1999. 'On the Spatial and Temporal
781 Links between Vegetation, Climate, and Soil Moisture'. *Water Resources Research* 35 (12):
782 3709–22. doi:10.1029/1999WR900255.

783 Rodríguez-Iturbe, I, and A. Porporato. 2007. *Ecohydrology of Water-Controlled Ecosystems: Soil*
784 *Moisture and Plant Dynamics*. Cambridge University Press.

785 Schwartz, B.F., M.E. Schreiber, and T. Yan. 2008. 'Quantifying Field-Scale Soil Moisture Using
786 Electrical Resistivity Imaging'. *Journal of Hydrology* 362 (3–4): 234–46.
787 doi:10.1016/j.jhydrol.2008.08.027.

788 Séger, M., I. Cousin, A. Frison, H. Boizard, and G. Richard. 2009. 'Characterisation of the Structural
789 Heterogeneity of the Soil Tilled Layer by Using in Situ 2D and 3D Electrical Resistivity
790 Measurements'. *Soil and Tillage Research* 103 (2): 387–398.

791 Seneviratne, S.I., T. Corti, E.L. Davin, M. Hirschi, E.B. Jaeger, I. Lehner, B. Orlowsky, and A. J. Teuling.
792 2010. 'Investigating Soil Moisture–climate Interactions in a Changing Climate: A Review'.
793 *Earth-Science Reviews* 99 (3–4): 125–61. doi:10.1016/j.earscirev.2010.02.004.

794 Shah, P.H., and D. N. Singh. "Generalized Archie's Law for Estimation of Soil Electrical Conductivity."
795 *Journal of ASTM International* 2, no. 5 (2005): 1–20.

796 Sidle, R.C., S. Noguchi, Y. Tsuboyama, and K. Laursen. 2001. 'A Conceptual Model of Preferential
797 Flow Systems in Forested Hillslopes: Evidence of Self-Organization'. *Hydrological Processes*
798 15 (10):1675–92. https://doi.org/10.1002/hyp.233.
799

800 Singha, K, and S.M. Gorelick. 2006. 'Effects of Spatially Variable Resolution on Field-Scale Estimates
801 of Tracer Concentration from Electrical Inversions Using Archie's Law'. *GEOPHYSICS* 71 (3):
802 G83–91. doi:10.1190/1.2194900.

803 Soulsby, C., C. Birkel, J. Geris, J. Dick, C. Tunaley, and D. Tetzlaff. 2015. 'Stream Water Age
804 Distributions Controlled by Storage Dynamics and Nonlinear Hydrologic Connectivity:
805 Modelling with High-Resolution Isotope Data: stream water age controlled by storage and
806 connectivity'. *Water Resources Research* 51 (9): 7759–76. doi:10.1002/2015WR017888.

807 Soulsby, C., J. Dick, B. Scheliga, and D. Tetzlaff. 2017. 'Taming the Flood - How Far Can We Go with
808 Trees?' *Hydrological Processes*, May. doi:10.1002/hyp.11226.

809 Soulsby, C., J. Bradford, J. Dick, J. P. McNamara, J. Geris, J. Lessels, M. Blumstock, and D. Tetzlaff.
810 2016. 'Using Geophysical Surveys to Test Tracer-Based Storage Estimates in Headwater
811 Catchments.: Geophysical Surveys to Test Tracer-Based Storage Estimates'. *Hydrological*
812 *Processes*, April. doi:10.1002/hyp.10889.

813 Soulsby, C., D. Tetzlaff, N. van den Bedem, I.A. Malcolm, P.J. Bacon, and A.F. Youngson. 2007.
814 'Inferring Groundwater Influences on Surface Water in Montane Catchments from
815 Hydrochemical Surveys of Springs and Streamwaters'. *Journal of Hydrology* 333 (2–4): 199–
816 213. doi:10.1016/j.jhydrol.2006.08.016.

817 Soulsby, C., H. Braun, M. Sprenger, M. Weiler, and D. Tetzlaff. "Influence of Forest and Shrub
818 Canopies on Precipitation Partitioning and Isotopic Signatures." *Hydrological Processes*, n.d.,
819 n/a-n/a. doi:10.1002/hyp.11351.

820 Sprenger, M, D. Tetzlaff, and C. Soulsby. 2017. 'Stable Isotopes Reveal Evaporation Dynamics at the
821 Soil-Plant-Atmosphere Interface of the Critical Zone'. *Hydrology and Earth System Sciences*
822 *Discussions*, February, 1–37. doi:10.5194/hess-2017-87.

823 Stephenson, N.L. 1990. ‘Climatic Control of Vegetation Distribution: The Role of the Water Balance’.
824 *The American Naturalist* 135 (5): 649–670.

825 Stewart, G, and A. C. Hull. 1949. ‘Cheatgrass (Bromus Tectorum L.)--An Ecologic Intruder in Southern
826 Idaho’. *Ecology* 30 (1): 58–74. doi:10.2307/1932277.

827 Srayeddin, I., and C. Doussan. “Estimation of the Spatial Variability of Root Water Uptake of Maize
828 and Sorghum at the Field Scale by Electrical Resistivity Tomography.” *Plant and Soil* 319, no.
829 1–2 (2009): 185–207.

830 Tetzlaff, D, C. Birkel, J. Dick, J. Geris, and C. Soulsby. 2014. ‘Storage Dynamics in Hydropedological
831 Units Control Hillslope Connectivity, Runoff Generation, and the Evolution of Catchment
832 Transit Time Distributions’. *Water Resources Research* 50 (2): 969–985.

833 Teuling, A.J., R. Uijlenhoet, F. Hupet, and P.A. Troch. 2006. ‘Impact of Plant Water Uptake Strategy
834 on Soil Moisture and Evapotranspiration Dynamics during Drydown’. *Geophysical Research*
835 *Letters* 33 (3). doi:10.1029/2005GL025019.

836 Toba, T., and T. Ohta. 2005. ‘An Observational Study of the Factors That Influence Interception Loss
837 in Boreal and Temperate Forests’. *Journal of Hydrology* 313 (3): 208–220.

838 Tomaškovičová, S., T. Ingeman-Nielsen, A. Christiansen, I. Brandt, T. Dahlin, and B. Elberling. “Effect
839 of Electrode Shape on Grounding Resistances — Part 2: Experimental Results and
840 Cryospheric Monitoring.” *GEOPHYSICS* 81, no. 1 (January 1, 2016): WA169-WA182.
841 doi:10.1190/geo2015-0148.1.

842 Topp, G. C., S. J. Zegelin, and I. White. 1994. ‘Monitoring Soil Water Content Using TDR: An Overview
843 of Progress’. In *Proc. Symp. Workshop Time Domain Reflectometry Environ., Infrastructure,*
844 *Mining Appl.*, 67–80. https://publications.csiro.au/rpr/pub?list=BRO&pid=procite:b202617e-
845 44da-4ac8-849f-2211a581609b.

Vereecken, H., J. A. Huisman, H. Bogena, J. Vanderborght, J. A. Vrugt, and J. W. Hopmans. 2008. 'On the Value of Soil Moisture Measurements in Vadose Zone Hydrology: A Review: SOIL MOISTURE AND HYDROLOGY'. *Water Resources Research* 44 (4): n/a-n/a. doi:10.1029/2008WR006829.

Vereecken, H, A. Binley, G. Cassiani, A. Revil, and K. Titov. 2006. 'APPLIED HYDROGEOPHYSICS'. In *Applied Hydrogeophysics*, 71:1–8. Dordrecht: Springer Netherlands. http://link.springer.com/10.1007/978-1-4020-4912-5_1.

Wang, H, D. Tetzlaff, J.J. Dick, and C. Soulsby. 2017. 'Assessing the Environmental Controls on Scots Pine Transpiration and the Implications for Water Partitioning in a Boreal Headwater Catchment'. *Agricultural and Forest Meteorology* 240: 58–66.

Warren, R.K. 2015. 'Examining the Spatial Distribution of Soil Moisture and Its Relationship to Vegetation and Permafrost Dynamics in a Subarctic Permafrost Peatland'.

Whalley, William R., A. Binley, C. W. Watts, Peter Shanahan, Ian Charles Dodd, E. S. Ober, R. W. Ashton, C. P. Webster, R. P. White, and Malcolm J. Hawkesford. "Methods to Estimate Changes in Soil Water for Phenotyping Root Activity in the Field." *Plant and Soil*, 2017, 1–16.

Zhou, Q.Y., J. Shimada, and A. Sato. 2001. 'Three-Dimensional Spatial and Temporal Monitoring of Soil Water Content Using Electrical Resistivity Tomography'. *Water Resources Research* 37 (2): 273–85. doi:10.1029/2000WR900284.

Zonge, K., J. Wynn, and S. Urquhart. "9. Resistivity, Induced Polarization, and Complex Resistivity." In *Near-Surface Geophysics*, 265–300. Investigations in Geophysics. Society of Exploration Geophysicists, 2005. doi:10.1190/1.9781560801719.ch9.

Zreda, M, D. Desilets, T. P. A. Ferré, and Russell L. Scott. 2008. 'Measuring Soil Moisture Content Non-Invasively at Intermediate Spatial Scale Using Cosmic-Ray Neutrons'. *Geophysical Research Letters* 35 (21). http://onlinelibrary.wiley.com/doi/10.1029/2008GL035655/full.

870 Zribi, M, T. Paris Anguela, B. Duchemin, Z. Lili, W. Wagner, S. Hasenauer, and Abdelghani Chehbouni.
871 2010. 'Relationship between Soil Moisture and Vegetation in the Kairouan Plain Region of
872 Tunisia Using Low Spatial Resolution Satellite Data'. *Water Resources Research* 46 (6).
873 http://onlinelibrary.wiley.com/doi/10.1029/2009WR008196/full.

874

875 **Tables**

	Mean (m^3 m^{-3})	Coefficient of variation (m^3 m^{-3})
Heather	0.36	0.11
Forest	0.46	0.12

876 Table 1: Average and coefficient of variation of VSM measured using TDR probes during study period

877

878 **Figures**

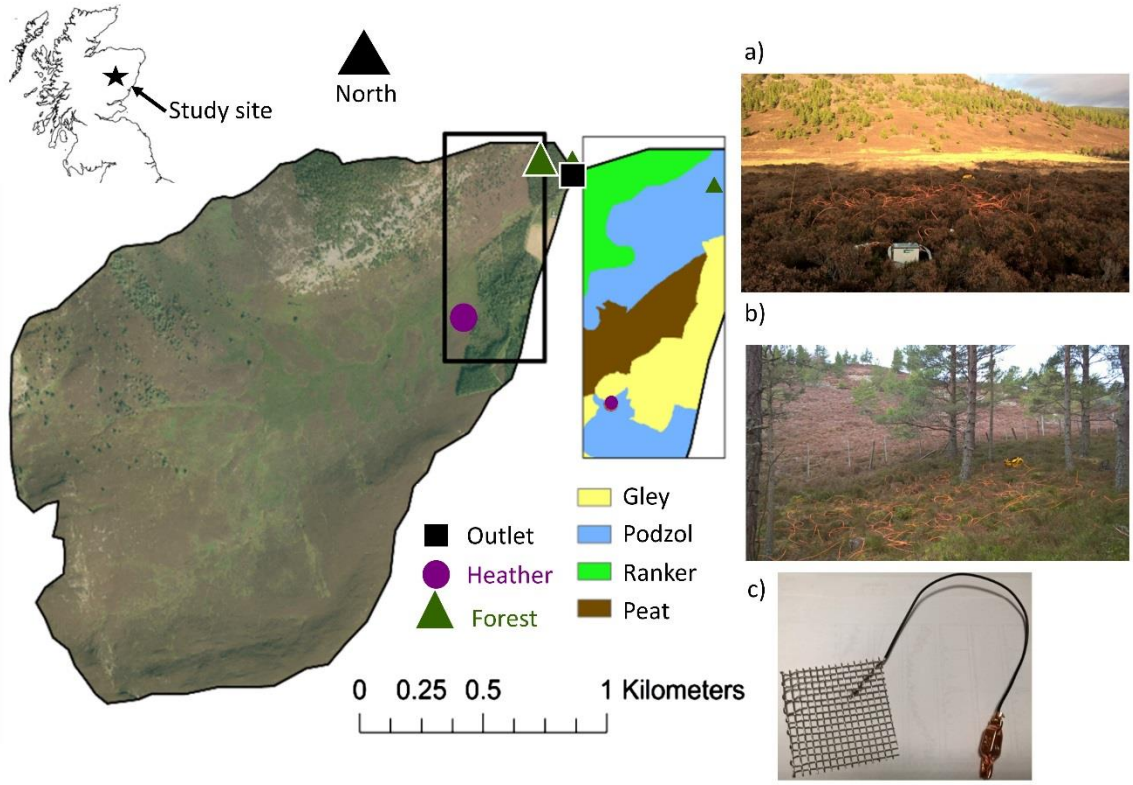

879

880 Fig. 1: Aerial image (1:12000) of Bruntland Burn catchment showing the heather and forest study
881 sites, and catchment outlet. Map insert (1:8500) shows soil type of the study sites. Inset
882 photographs show the field setting for the plots in the heather (a) and forest sites (b), respectively.
883 Photography c, shows the electrode design (5x5 cm).

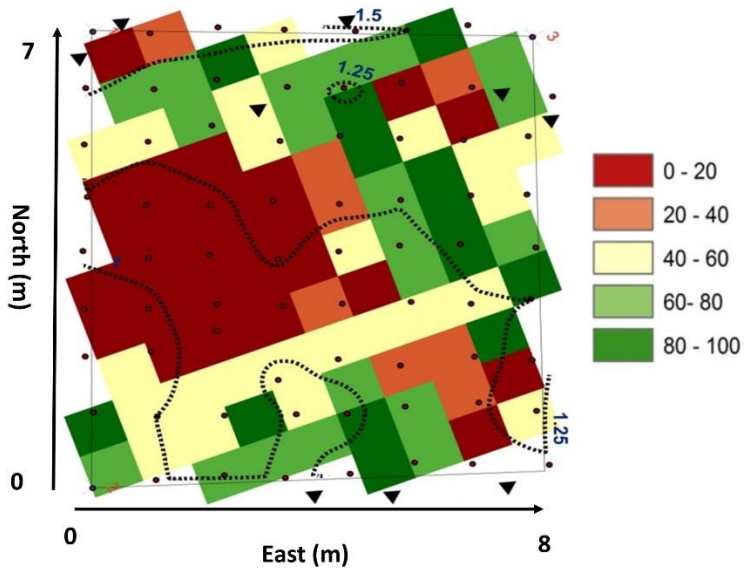

884

885 Fig. 2: Canopy cover (in %) and elevation (contour intervals: 0.25 m) relative to point (0, 0) for the

886 forest site. Black triangles indicate tree locations.

887

888

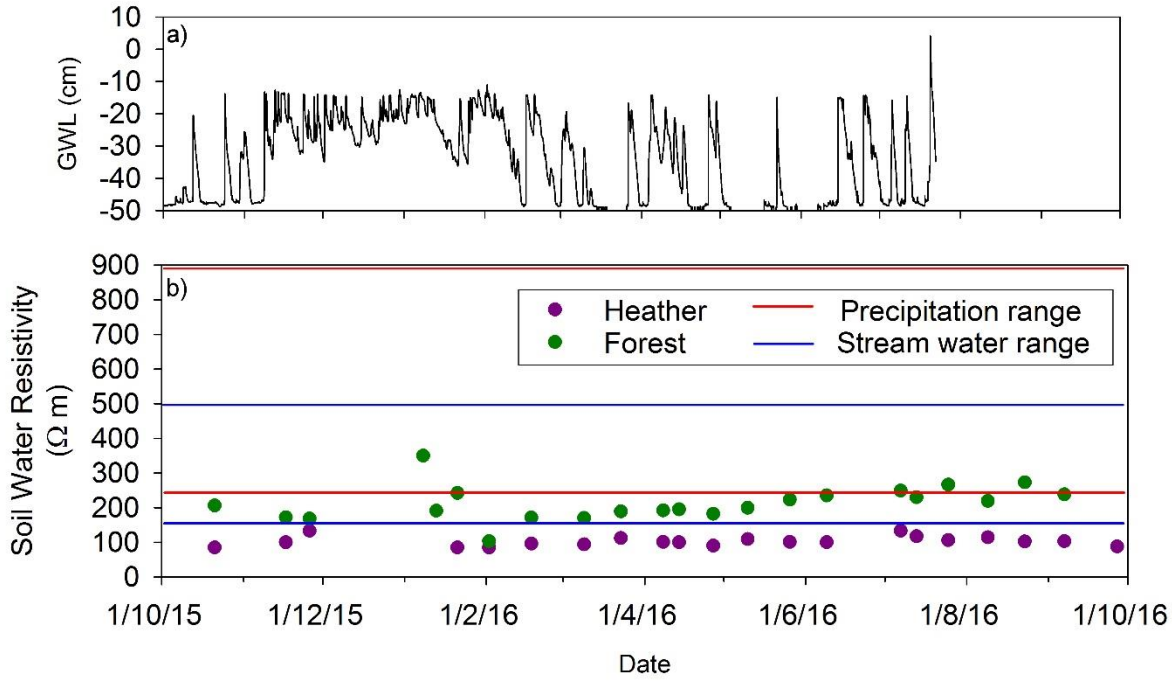

889

890 Fig. 3: a) Groundwater level (GWL) for the heather site, and b) estimated soil water resistivity values
891 for each survey at the heather and forest site. Lines indicate the measured precipitation and stream
892 water resistivity. Groundwater time-series at the heather site ends in late July due to logger failure.

893

894

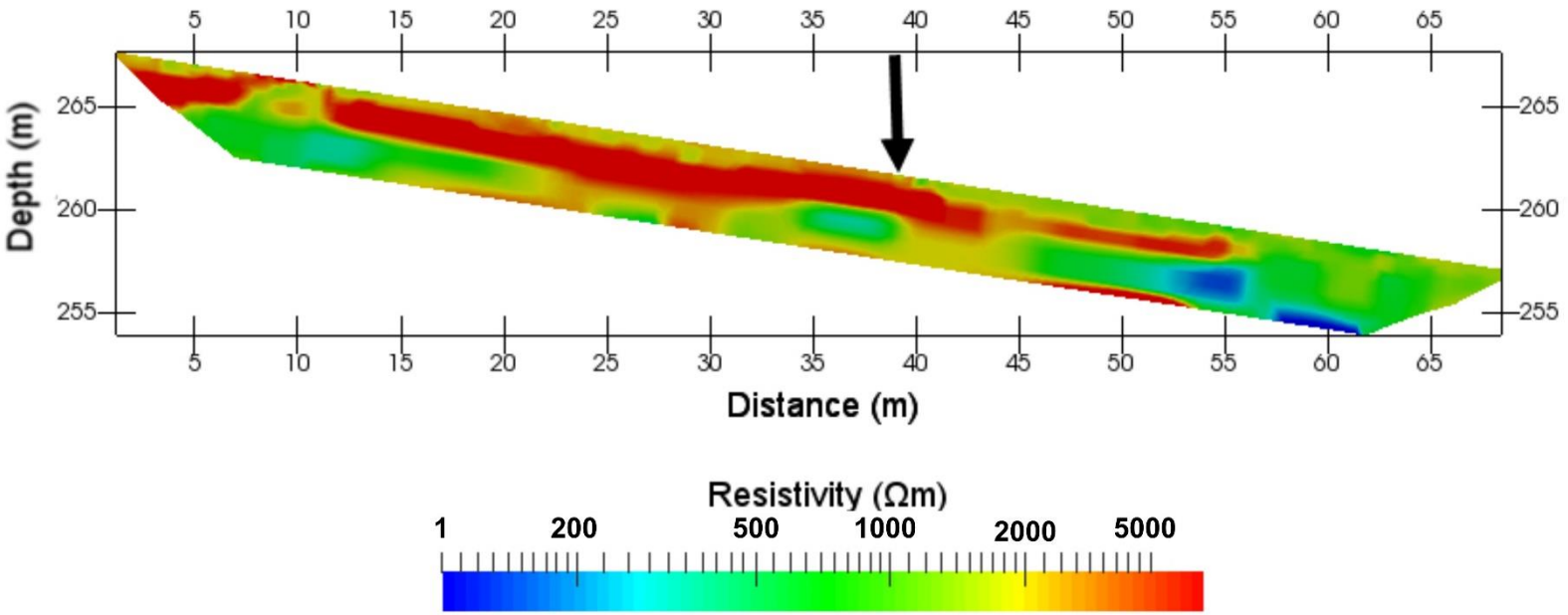

895

896 Fig. 4: Resistivity for the 72 m long transect through the forest hillslope, showing high resistivity scree material in the shallow subsurface. Black arrow

897 indicates location of plot and transect.

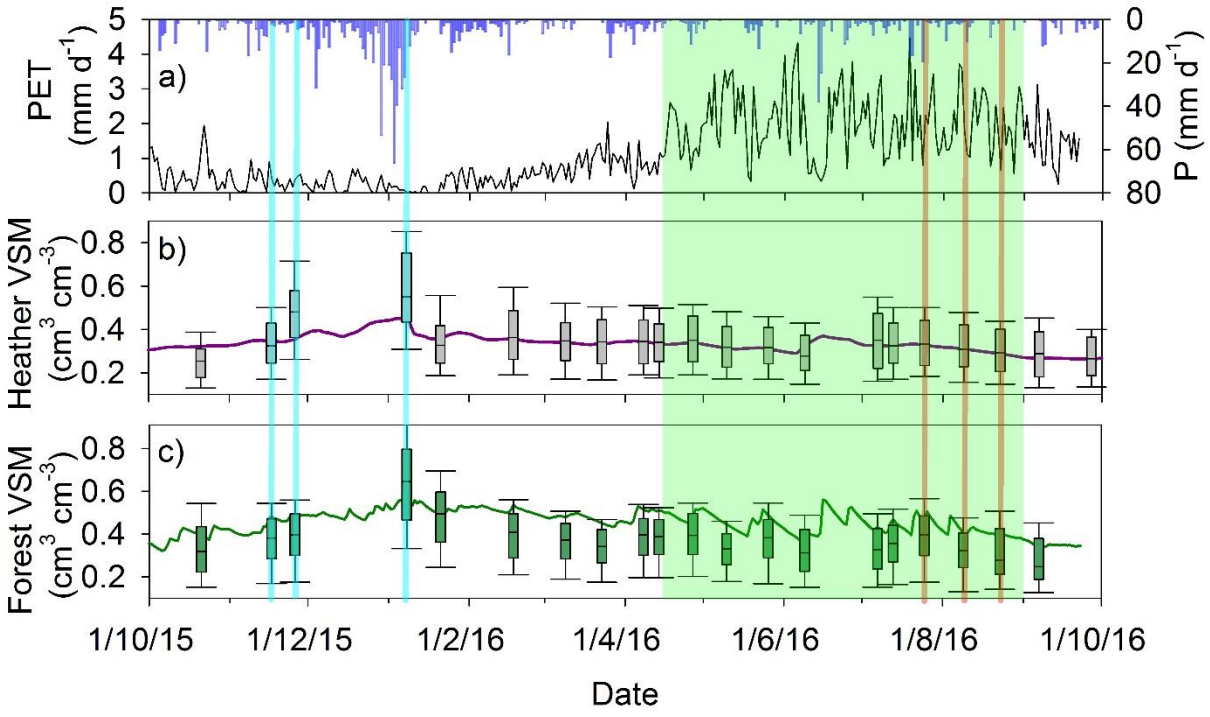

Fig. 5: Time series of: a) precipitation (P) and potential evapotranspiration (PET), b) VSM at the heather site, and c) VSM at the forest site. Solid lines in b and c represent the TDR measured VSM, and the box plots represent the mean, 5th, 25th, 75th, and 95th percentiles. Additionally, the blue and orange lines represent the periods of wetting and drying in Figure 7 respectively, and the green shading, the growing season.

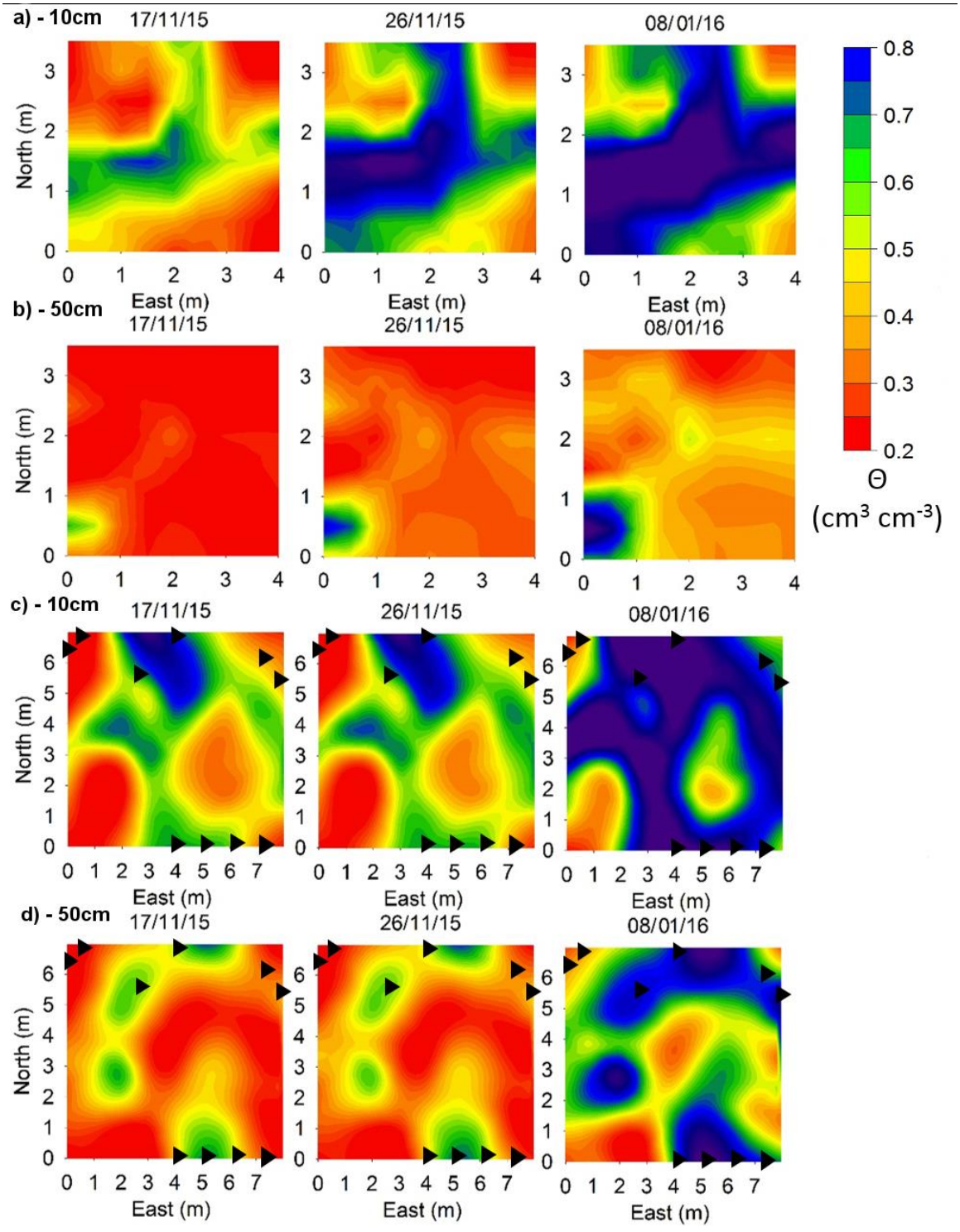

906

907 Fig. 6: Wetting cycle from 17/11/15 to 08/01/16 at the heather sites 0.1 m (a) and 0.5 m (b) depths,

908 and the forest sites 0.1 m (c) and 0.5 m (d) depths. Black triangles are tree locations.

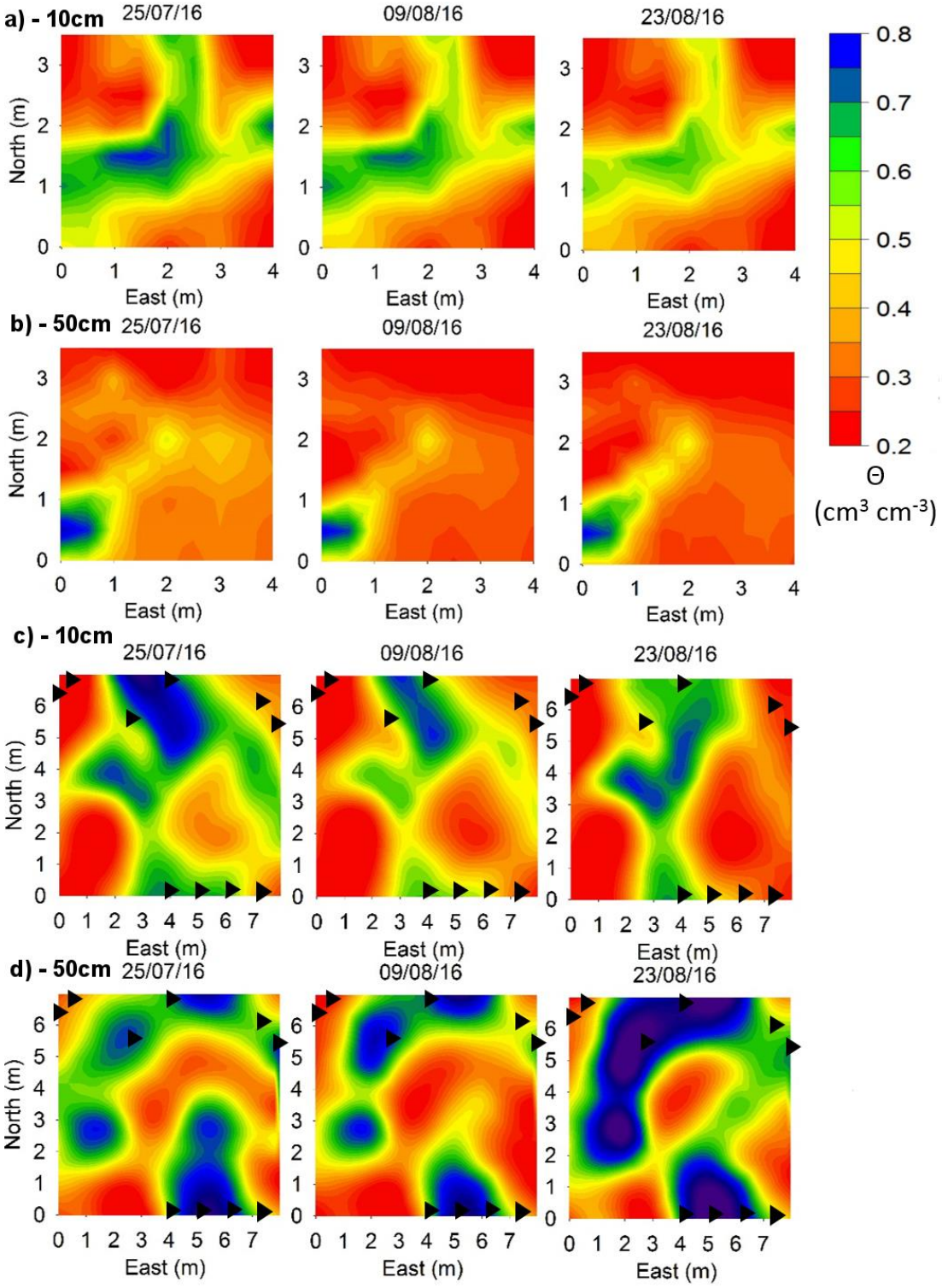

909

910 Fig. 7: Drying cycle from 25/07/16 to 23/08/16 at the heather sites 0.1 m (a) and 0.5 m (b) depths,

911 and the forest sites 0.1 m (c) and 0.5 m (d) depths. Black triangles are tree locations.

912

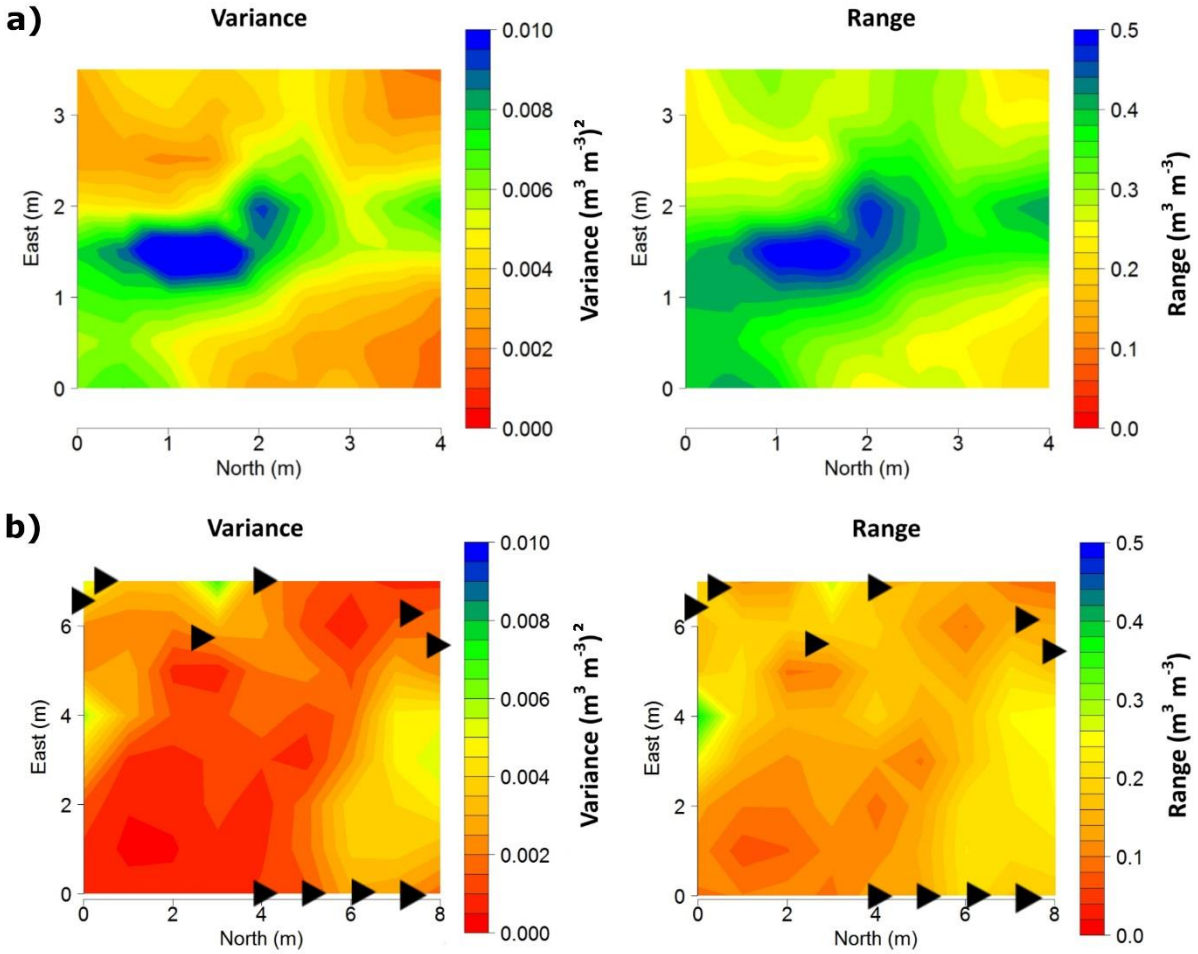

913

914 Fig. 8: Plots for temporal variance and range of VSM at 0.1 m depth for a) heather and b) forest sites.

915

916

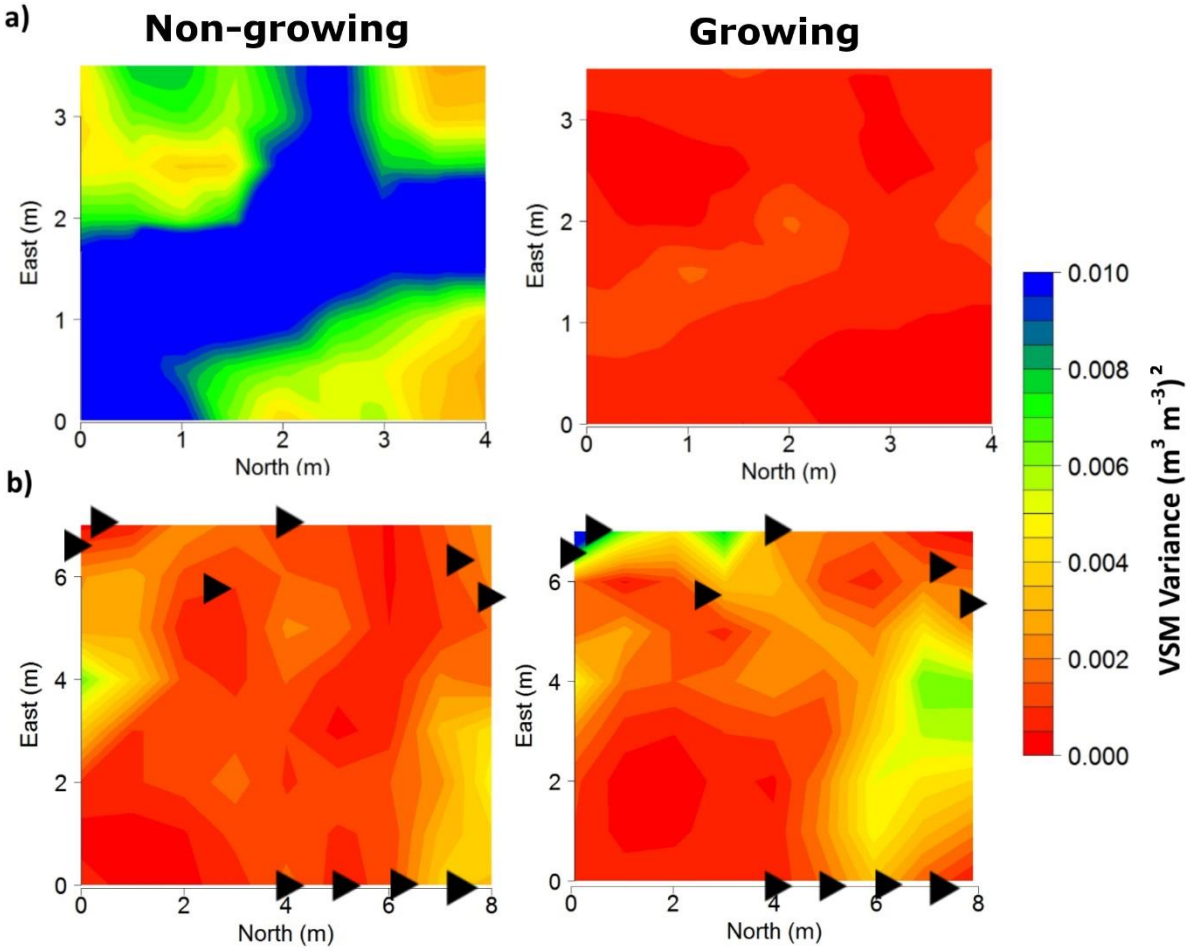

917

918 Fig. 9: VSM temporal variance plots for 0.1 m depth for the growing and non-growing season for a)

919 the heather site and b) the forest site.

920

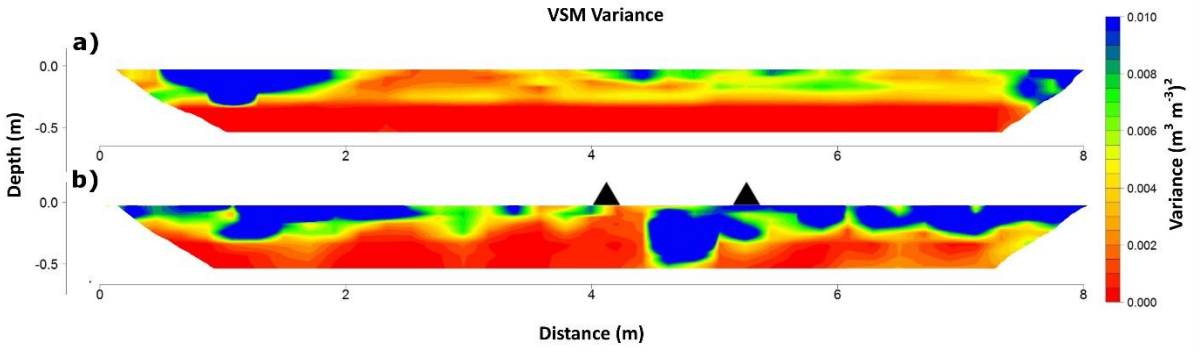

Fig. 10: Transects showing, a) the VSM statistical temporal variance between surveys for the heather site, and, b) the VSM statistical temporal variance between surveys for the forest site, Black triangles show position of scots pine.

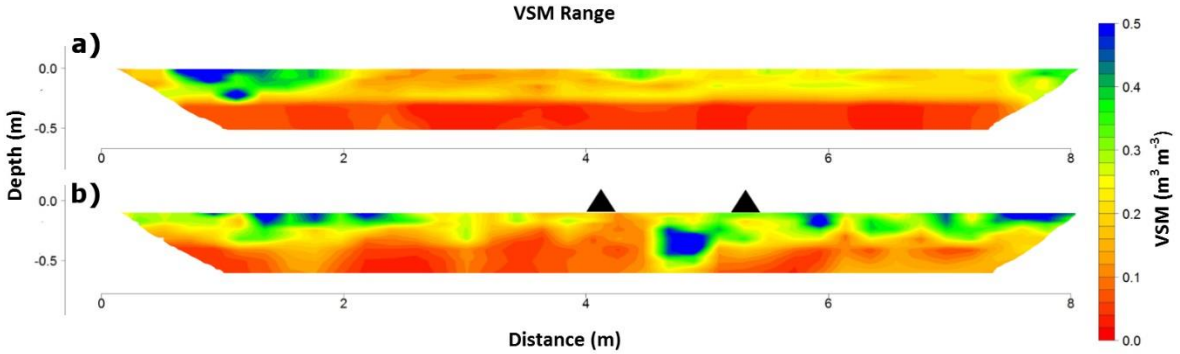

Fig. 11: Transects showing, a) the range of VSM temporal change between surveys for the heather site, and, b) range of VSM temporal change between surveys for the forest site. Black triangles show position of scots pine.